PFM of Piezoelectric Materials: Contact Mechanics and Resolution Theory

Sergei V. Kalinin

The Center for Nanophase Materials Sciences and
Materials Sciences and Technology Division
Oak Ridge National Laboratory,

Piezoresponse Force Microscopy

5.1. Contact mechanics of PFM

5.1.1. Exact solutions

5.1.2. Decoupled approximation

5.1.3. Implications for imaging

5.2. Resolution theory in PFM

5.2.1. Resolution and Information limit

5.2.2. Tip calibration

5.2.3. Image reconstruction

Probing NanoElectromechanics

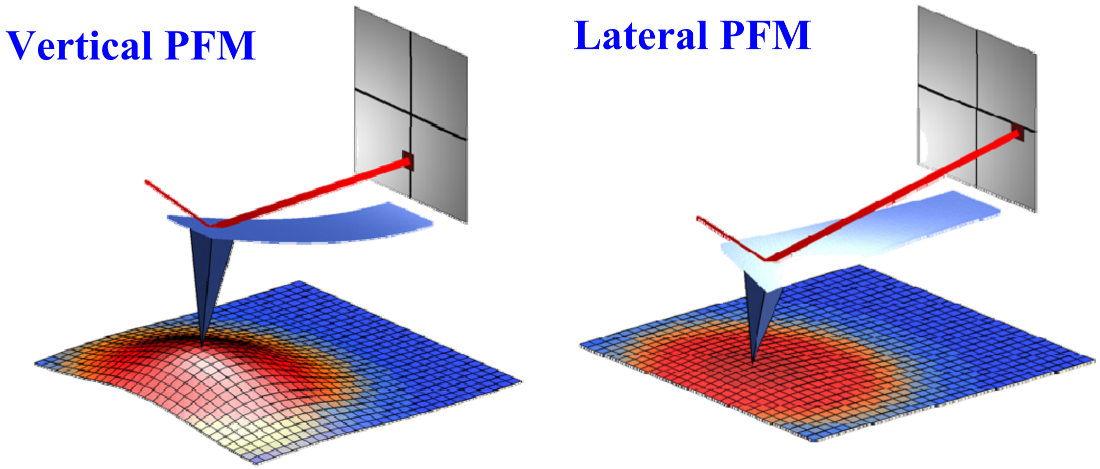

Piezoresponse Force Microscopy

Application of AC bias to the tip

$$V_{tip} = V_{dc} + V_{ac}\cos(\omega t)$$

results in cantilever deflection

$$d = d_0 + A(\omega, V_{dc})V_{ac}\cos(\omega t + \varphi)$$

due to piezoelectric effect

PFM = Nanoelectromechanics

Image formation in PFM

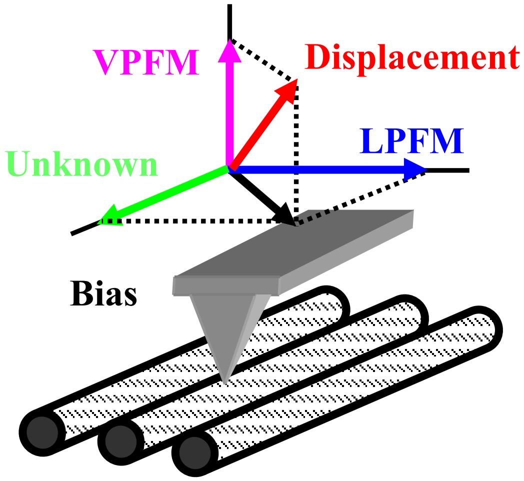

Several competing contributions:

1. Vertical surface response
2. Longitudinal response
3. Torsional response
4. Local electrostatic force
5. Distributed electrostatic force

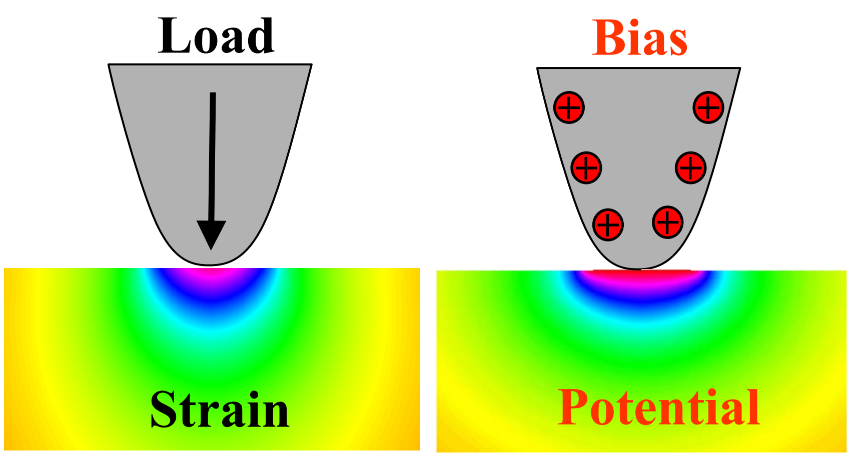

In piezoelectric materials, electrical and mechanical phenomena are coupled

1. **Tip-surface contact mechanics**
   - origins of PFM signal
2. Cantilever dynamics
   - Detection mechanism
3. **Field structure in material**
   - Resolution
   - hysteresis measurements
   - switching phenomena

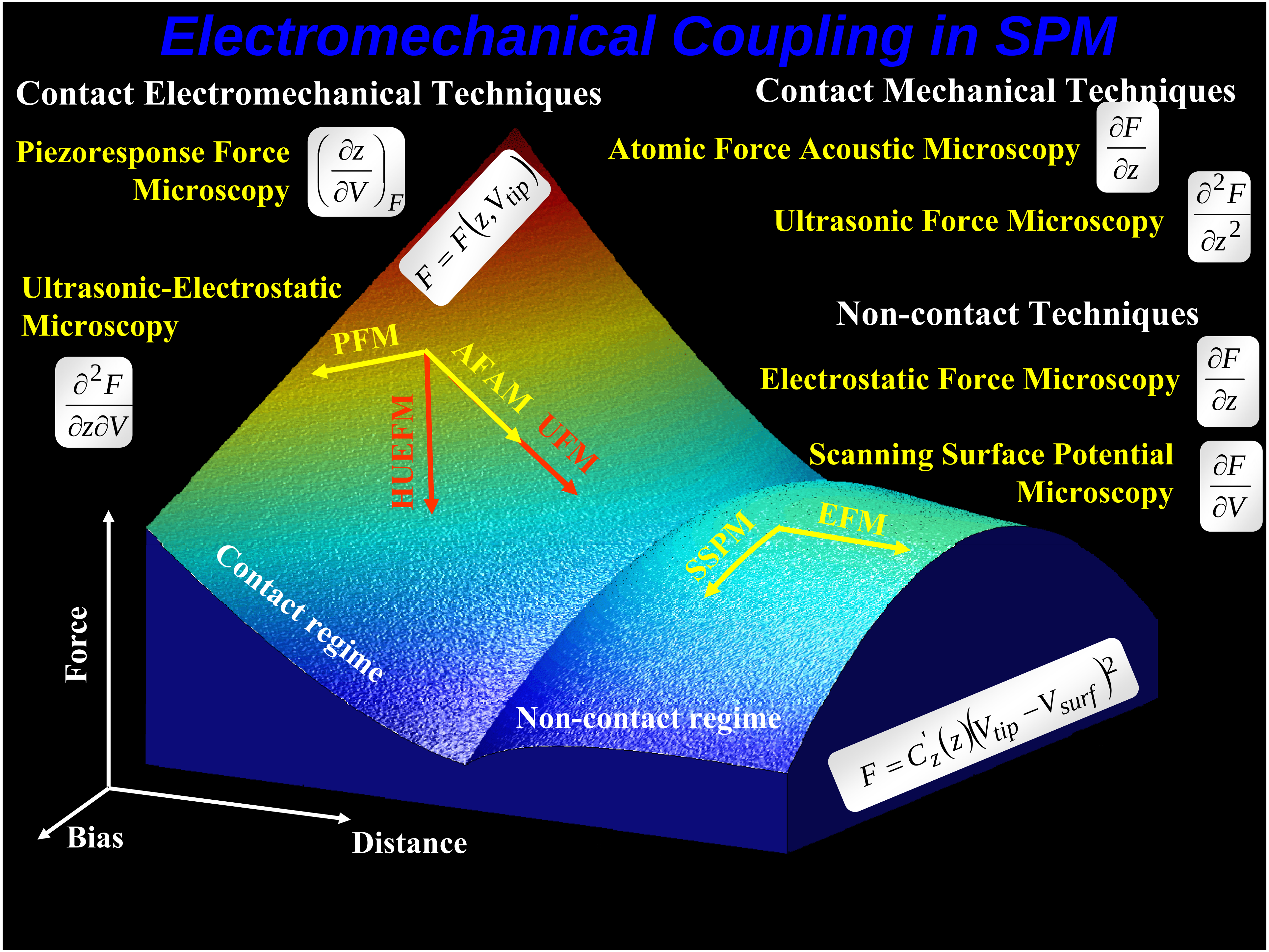
Electromechanical Coupling in SPM
Contact Electromechanical Techniques
Contact Mechanical Techniques
Piezoresponse Force Microscopy
$\left(\frac{\partial z}{\partial V}\right)_F$
Atomic Force Acoustic Microscopy
$\frac{\partial F}{\partial z}$
Ultrasonic Force Microscopy
$\frac{\partial^2 F}{\partial z^2}$
$F = F(z, V_{tip})$
Ultrasonic-Electrostatic Microscopy
$\frac{\partial^2 F}{\partial z \partial V}$
Non-contact Techniques
Electrostatic Force Microscopy
$\frac{\partial F}{\partial z}$
Scanning Surface Potential Microscopy
$\frac{\partial F}{\partial V}$
PFM
AFAM
UFM
HUEFM
SSPM
EFM
Contact regime
Non-contact regime
$F = C'_z(z)(V_{tip} - V_{surf})^2$
Force
Bias
Distance

Piezoresponse Force Microscopy of Materials with Out-of-Plane Polarization

Examples: c^+-c^- domains in $BaTiO_3$, periodically poled $LiNbO_3$, poled polymers

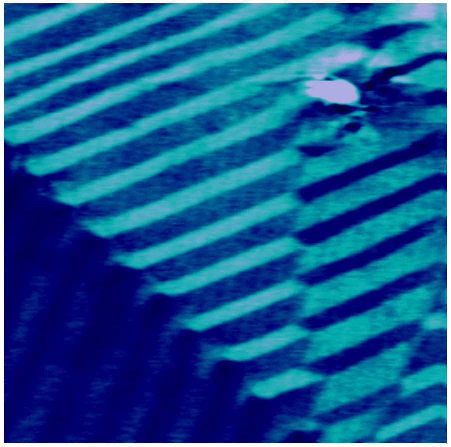

$BaTiO_3$

Poled $LiNbO_3$

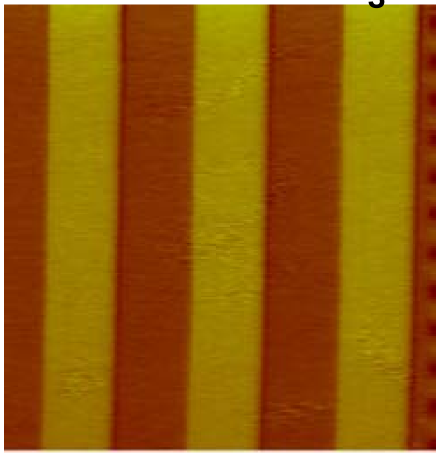

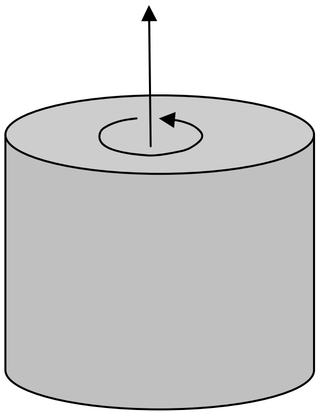

For piezoelectric and elastic properties, tetragonal and hexagonal symmetries are equivalent to transversally isotropic

- *The highest symmetry possible for ferroelectric material*
- *No lateral response component*
- *A rigorous electromechanical solution exists!*
- *Starting point to more complex systems*

Nanoelectromechanics of PFM

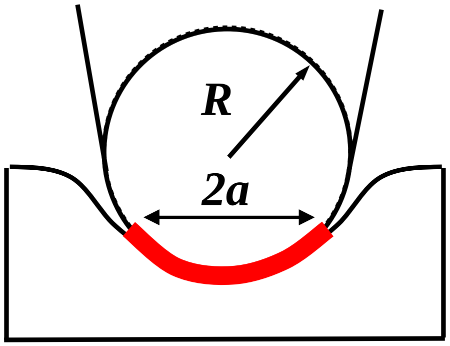

1872: Hertz – spherical indentation of isotropic material

1945: Sneddon – arbitrary indentor shape

1992: Hanson: transversally isotropic material

2002: Karapetian and Kachanov: piezoelectric material

Stiffness Relations

Indentation depth: $w_0 = \dfrac{a^2}{R}$

Load: $P = \dfrac{4a^3 C_1^*}{3\pi R} + \dfrac{2a\psi_0 C_3^*}{\pi}$

Charge: $Q = -\dfrac{4a^3 C_3^*}{3\pi R} + \dfrac{2a\psi_0 C_4^*}{\pi}$

a – indentation radius, R – tip radius

C_1^* **Indentation elastic stiffness**

C_3^* **Indentation piezoelectric coefficient**

C_4^* **Indentation dielectric constant**

This is the first rigorous solution of spherical indentation problem for piezoelectric material in analytical functions.

S.V. Kalinin, E. Karapetian, and M. Kachanov, Phys. Rev. **B,** 2004

E. Karapetian, M. Kachanov, and S.V. Kalinin, Phil. Mag. 2005

Nanoelectromechanics for Arbitrary Indentor

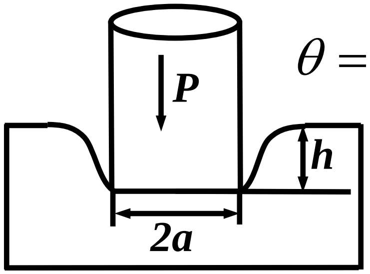

$\theta = a$

Flat: $n = 0$

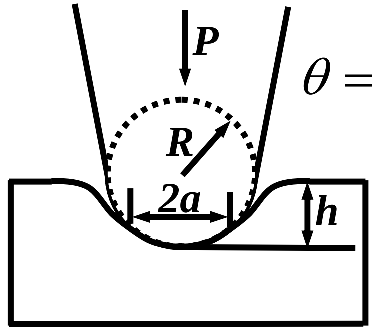

$\theta = \dfrac{2R^{1/2}}{3}$

Spherical: $n = 1/2$

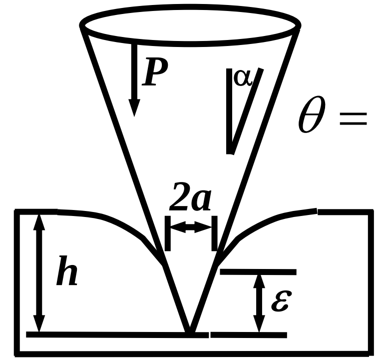

$\theta = \dfrac{\tan\alpha}{\pi}$

Conical: $n = 1$

Load: $P = \dfrac{2}{\pi}\theta\left(h^{n+1}C_1^* + (n+1)h^n\psi_0 C_3^*\right)$

Charge: $Q = \dfrac{2}{\pi}\theta\left(-h^{n+1}C_3^* + (n+1)h^n\psi_0 C_4^*\right)$

For uniform field:

$h = d_{33}V$

$Q = d_{33}F$

Implications:

1. In the SPM or indentation experiment, we can determine only indentation moduli, but not the individual elements of elastic, piezoelectric or dielectric tensors
2. In contact problem, indentor shape function and materials properties are decoupled, hence the indentor can be calibrated
3. Experimentally, we can measure C_3/C_1 by PFM and C_1 by e.g. Atomic Force Acoustic Microscopy. In SPM, due to smallness of capacitance, C_4 can not be measured directly

Materials Properties and Effective Response

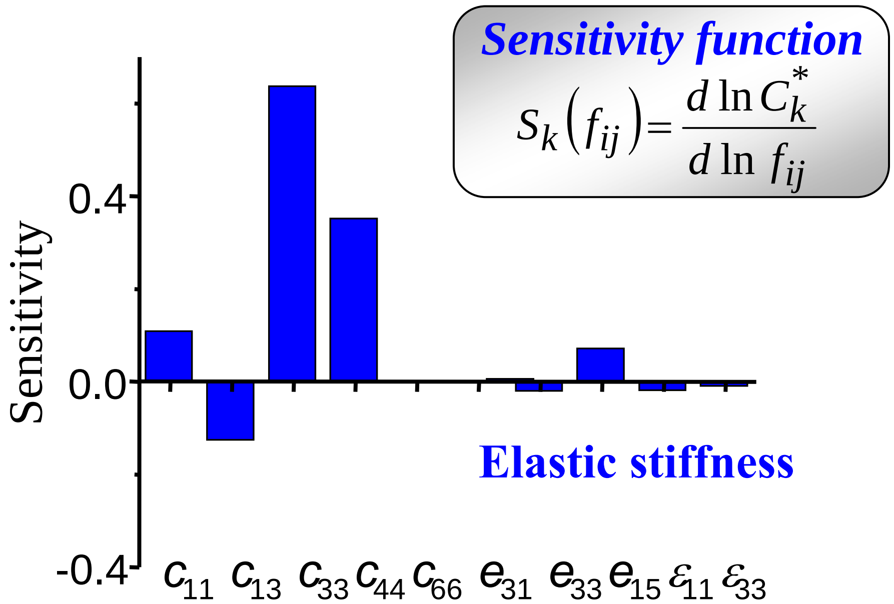

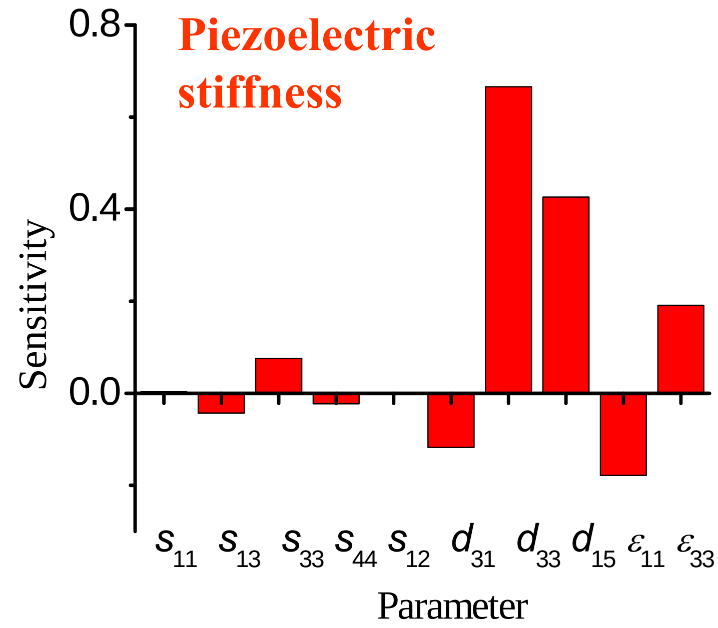

Indentation stiffnesses are complex functions of materials properties:

$$C_i^* = C_i^*\left(c_{ij}, d_{ij}, \varepsilon_{ij}\right)$$

- Elastic indentation module is determined primarily by c_{ij}
- PFM signal is determined by d_{ij} and ε_{ij}
- Dielectric properties are determined by ε_{ij}

Materials Properties and Effective Response

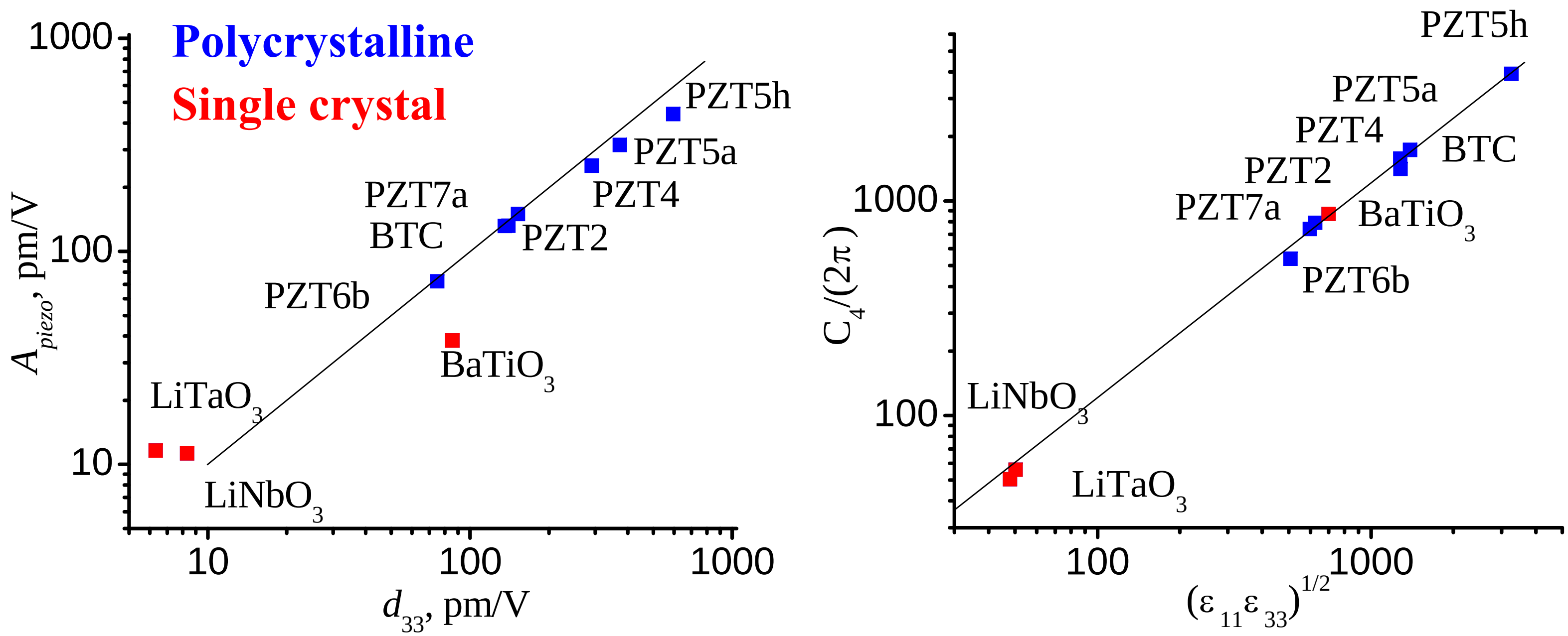

- Piezoresponse amplitude is a complex function of materials constants
- There is a reasonable correlation between PFM signal and d_{33}
- Indentor charge can be obtained from simple theory

Implications for Electromechanical and Mechanical SPM

$$P = \frac{2}{\pi}\theta\left(h^{n+1}C_1^* + (n+1)h^n V_{tip} C_3^*\right)$$

In Piezoresponse Force Microscopy, measured is Independent of tip geometry

$$d_{eff} = \frac{\partial h}{\partial V_{tip}} = \frac{C_3^*}{C_1^*}$$

In Atomic Force Acoustic Microscopy, signal is related to tip-surface spring constant.

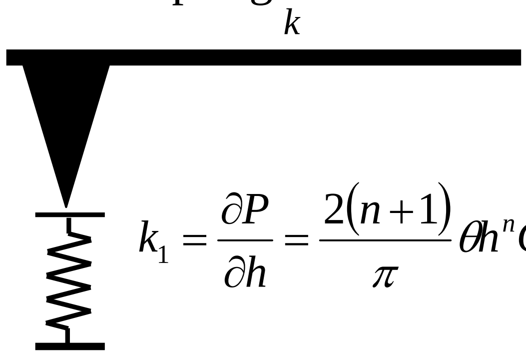

$$k_1 = \frac{\partial P}{\partial h} = \frac{2(n+1)}{\pi}\theta h^n C_1^*$$

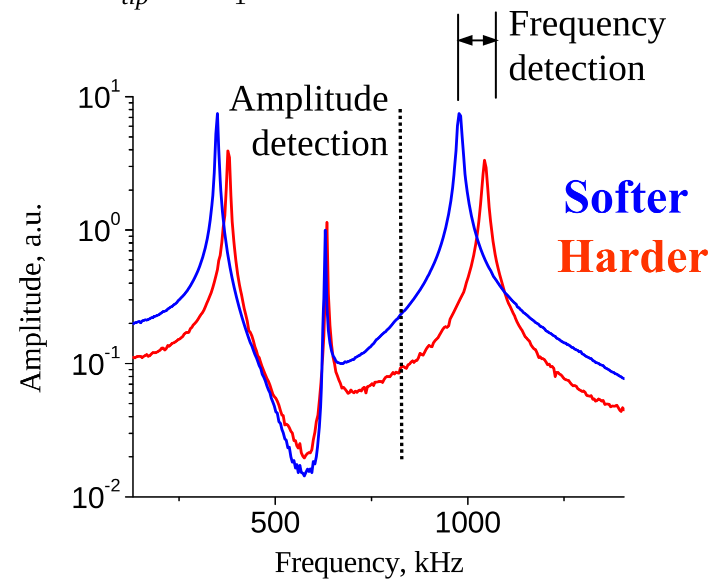

Positive: PFM signal is independent on tip geometry and topography

Negative: we can not use resonant enhancement in PFM

Approximate Theory for PFM

Rigorous solution is limited:

- Ignores fields outside the contact area (classical limit)
- Limited to transversally-isotropic material
  - no lateral PFM
  - no materials other then (100) surfaces of hexagonal perovskites
- Can not be used to describe PFM signal in
  - thin films
  - nanoparticles
  - domain wall profiles
  - cylindrical domains (PFM spectroscopy)

We need approximate solutions!

Green's Function Model

From rigorous solution, we know that far from contact, fields rapidly approach that for point charge/point force

Rigorous solution: For fully anisotropic materials, the Green's function for point charge/point force for coupled electromechanical problem has recently been derived using linear plane wave method. (V. Borovikov, 2005)

- Arbitrary materials symmetry
  - Can describe vertical and lateral PFM
- Unphysical singularity at origin
  - can not describe switching and spectroscopy
- Ignores effects of tip shape, contact vs. non-contact contributions, etc.

Decoupled Green's Function Model

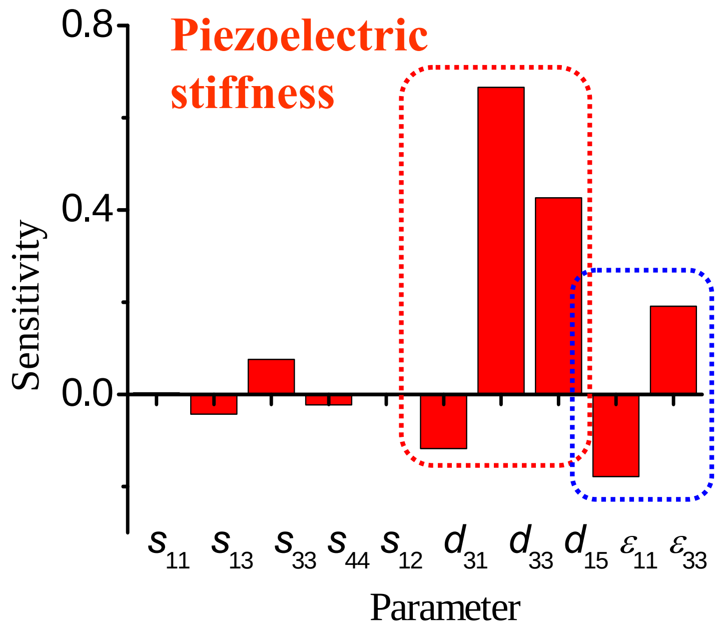

The sensitivity analysis of exact solution suggests that approximate solution can be found as

$$u_3(\mathbf{x}) = d_{33} f_1(\varepsilon_{11}/\varepsilon_{33}) + d_{15} f_2(\varepsilon_{11}/\varepsilon_{33}) + d_{31} f_3(\varepsilon_{11}/\varepsilon_{33})$$

For general anisotropy

$$u_i(\mathbf{x}) = \sum_{jk} d_{ijk} f_{jk}(\varepsilon_{11}/\varepsilon_{33})$$

Decoupled approximation

- Calculate electric field for rigid dielectric, $d_{ijk} = 0$
- Calculate stress field using piezoelectric constitutive equations, $X_{ij} = E_k d_{kij}$
- Calculate displacement field using Green's function for non-piezoelectric elastic solid

$$u_i(\mathbf{x}) = \int_0^{\infty} d\xi_3 \int_{-\infty}^{\infty} d\xi_2 \int_{-\infty}^{\infty} d\xi_1 \frac{\partial G_{ij}(\mathbf{x},\xi)}{\partial \xi_k} E_l(\xi) c_{kjmn} d_{lnm}$$

Decoupled Green's Function Model

Benefits of decoupled approximation:

• Can take into account any field structure (solve electrostatic problem)
• Arbitrary materials symmetry (as given by dielectric, piezoelectric, and elastic tensors)
• Can naturally be used to describe microstructural elements such as variations in elastic properties, domain walls, etc.
• Can be further simplified by assuming special materials symmetries for elastic and mechnical properties

Error estimate: From $D_i = d_{ijk} X_{jk} + \varepsilon_{im} E_m$ we get $E_k = \varepsilon_{ki}^{-1} D_i - \varepsilon_{ki}^{-1} d_{ijl} X_{jl}$

Substituting into $U_{ij} = s_{ijkl} X_{kl} + E_m d_{mij}$

we obtain $U_{ij} = \left(1 - s_{ijkl}^{-1} \varepsilon_{mp}^{-1} d_{plk} d_{mij}\right) s_{ijkl} X_{kl} + \varepsilon_{mp}^{-1} d_{mij} D_p$

$$k_{ij}^2 = \left(d_{ij}\right)^2 / \left(s_{jj} \varepsilon_{ii}\right)$$

$BaTiO_3$:	$k_{15}^2 \approx 0.32$	$k_{31}^2 \approx 0.10$	$k_{33}^2 \approx 0.31$
PZT:	$k_{15}^2 \approx 0.14$	$k_{31}^2 \approx 0.02$	$k_{33}^2 \approx 0.13$
Quartz:	$k_{11}^2 \approx 0.01$		

For most materials, error is of order of 10-30% or less!

Electric Field Structure

1. Represent tip using image charge series or multipole expansion

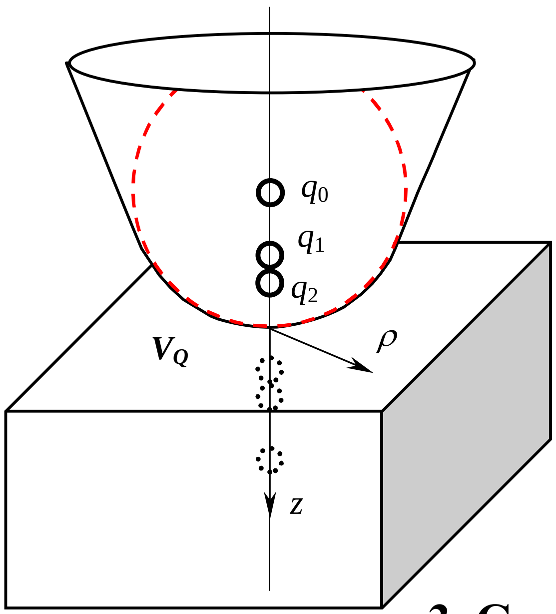

2. Solve Laplace's equation

$$\begin{cases} \varepsilon_0 \varepsilon_{ij} \dfrac{\partial^2}{\partial x_i \partial x_j} V(\mathbf{r}) = 0, \quad z \ge 0 \\ \varepsilon_0 \Delta V_0(\mathbf{r}) = -Q \cdot \delta(z+d)\delta(x)\delta(y), \quad z < 0 \end{cases}$$

with boundary conditions

$$\varepsilon_{3j} \frac{\partial}{\partial x_j} V(z=0) = \frac{\partial}{\partial z} V_0(z=0),$$

$$V(z=0) = V_0(z=0)$$

3. General answer

$$V(\mathbf{r}) = \frac{Q}{2\pi\varepsilon_0} \int_{-\infty}^{\infty} dk_x \int_{-\infty}^{\infty} dk_y \frac{\exp(-ik_x x - ik_y y)}{2\pi} \cdot \frac{\exp\left(-d\sqrt{k_x^2 + k_y^2} - z\lambda(k_x, k_y)\right)}{\left(\sqrt{k_x^2 + k_y^2} + (i\varepsilon_{31} k_x + i\varepsilon_{32} k_y + \varepsilon_{33}\lambda)\right)}$$

4. Transversally-isotropic

$$V_Q(\rho, z) = \frac{Q}{2\pi\varepsilon_0(\kappa+1)} \frac{1}{\sqrt{\rho^2 + (z/\gamma + d)^2}}$$

Dielectric constant $\kappa = \sqrt{\varepsilon_{33}\varepsilon_{11}}$

Dielectric anisotropy $\gamma = \sqrt{\varepsilon_{33}/\varepsilon_{11}}$

Elastic Green's function

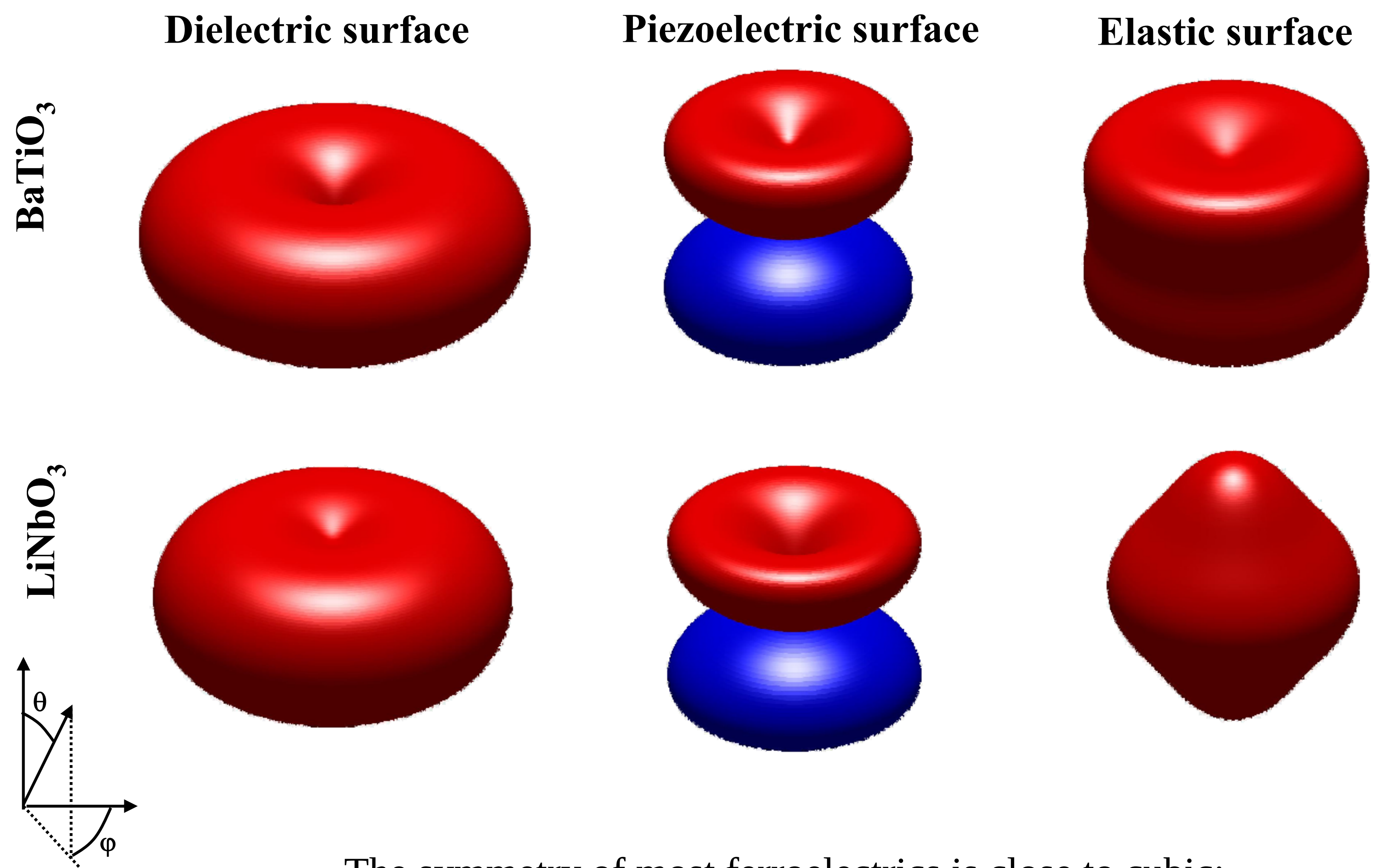

The symmetry of most ferroelectrics is close to cubic:
approximate elastic properties as isotropic!

Solution for Transversally Isotropic Material

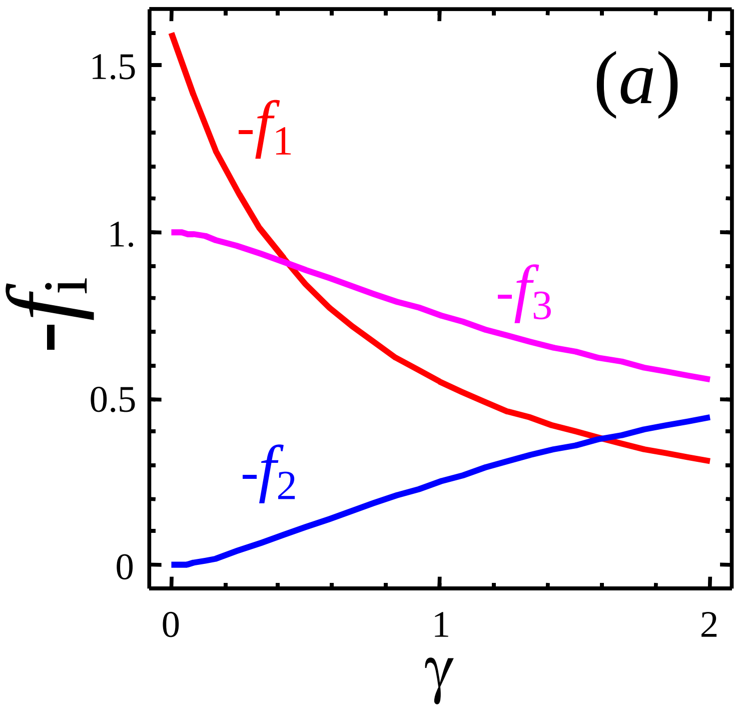

Surface displacement:

$$u_3(\rho) = \frac{Q}{2\pi\varepsilon_0(1+\kappa)} \frac{d_{31} f_1(\gamma) + d_{15} f_2(\gamma) + d_{33} f_3(\gamma)}{\sqrt{\rho^2 + d^2}},$$

where

$$f_1(\gamma) = -\frac{1 + 2(1+\gamma)\nu}{(1+\gamma)^2}$$

$$f_2(\gamma) = -\frac{\gamma^2}{(1+\gamma)^2}$$

$$f_3(\gamma) = -\frac{1+2\gamma}{(1+\gamma)^2}$$

Piezoresponse: $PR = d_{31} f_1(\gamma) + d_{15} f_2(\gamma) + d_{33} f_3(\gamma)$

Response Theorem 1: For a transversally isotropic piezoelectric solid in an isotropic elastic approximation and an arbitrary point charge distribution in the tip (not necessarily constrained to a single line), the vertical surface displacement is proportional to the surface potential induced by the tip in the point of contact

Solution for General Anisotropy

For anisotropic material: $u_i(\mathbf{x}) = V_Q(0) R_{ijlk}(\mathbf{x}) d_{klj}$

where $$R_{imnl}(\mathbf{x}) = \frac{1}{V_Q(0)} \int_0^{\infty} d\xi_3 \int_{-\infty}^{\infty} d\xi_2 \int_{-\infty}^{\infty} d\xi_1 \frac{\partial G_{ij}(\mathbf{x},\xi)}{\partial \xi_k} E_l(\xi) c_{kjmn}$$

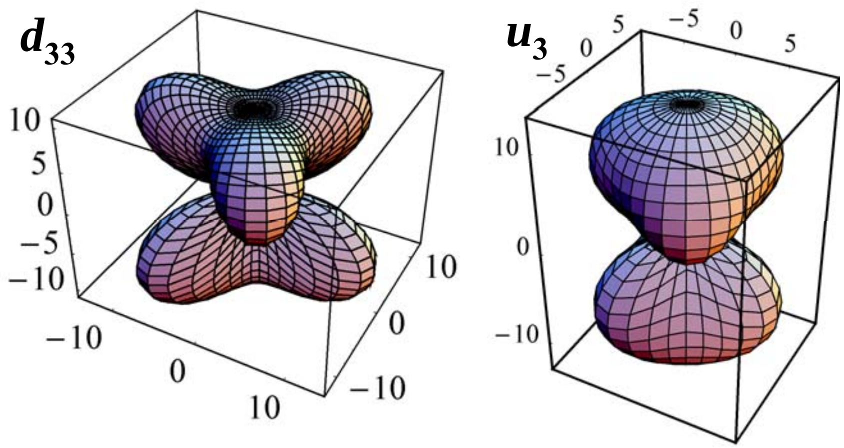

Piezoresponse surfaces for $LiNbO_3$

For isotropic material:

$$R_{121} = \frac{1-12\nu}{32}$$

$$R_{131} = -\frac{1}{8}$$

$$R_{111} = -\frac{13+4\nu}{32}$$

Response Theorem 2: For an anisotropic piezoelectric solid in the limit of dielectric and elastic isotropy, the vertical and lateral PFM signals are proportional to the potential on the surface induced by the tip if the tip charges and the point of contact are located on the same line along the surface normal.

Solutions for non-standard probes

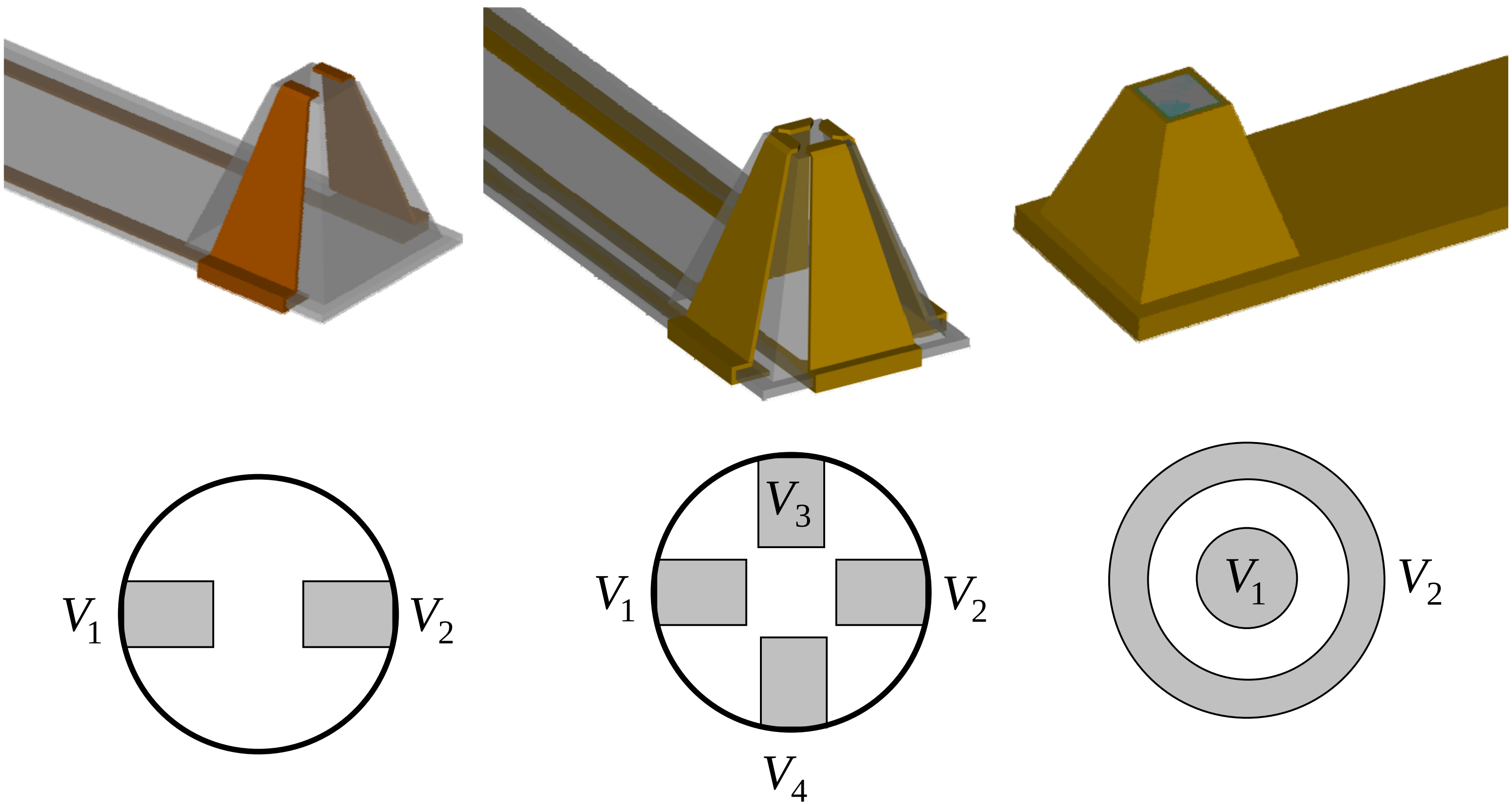

Strip-line **Quadrupole or rotating dipole** **Shielded probe**

Principles of Orientation Imaging

Experiment: measure the mechanical displacement in the applied electric field direction

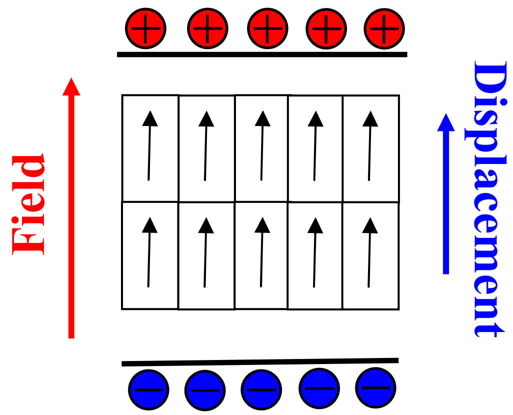

For tetragonal ferroelectric such as $BaTiO_3$, if the field is **parallel** to the c-axis, there is strong deformation of the crystal in the field direction

$$\delta z = d_{33} E_3 h \quad \text{or} \quad \delta z = 80V \text{ pm}$$

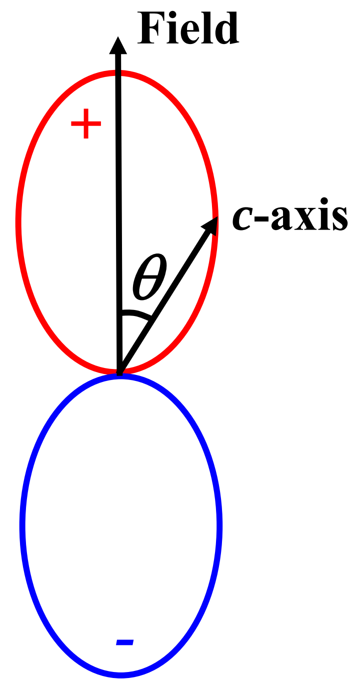

If the field is **perpendicular** to the c-axis, the deformation in the field direction is zero

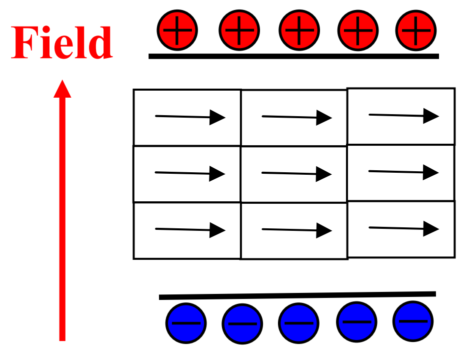

In the general case:

$$\delta z = (d_{15} + d_{31}) \sin^2 \theta \cos\theta + d_{33} \cos^3 \theta$$

From known electromechanical response, we can determine crystal orientation!

- small displacements (10-100 pm)
- spatially localized (< 1 μm)

Toward Single Molecule Imaging

Con Map

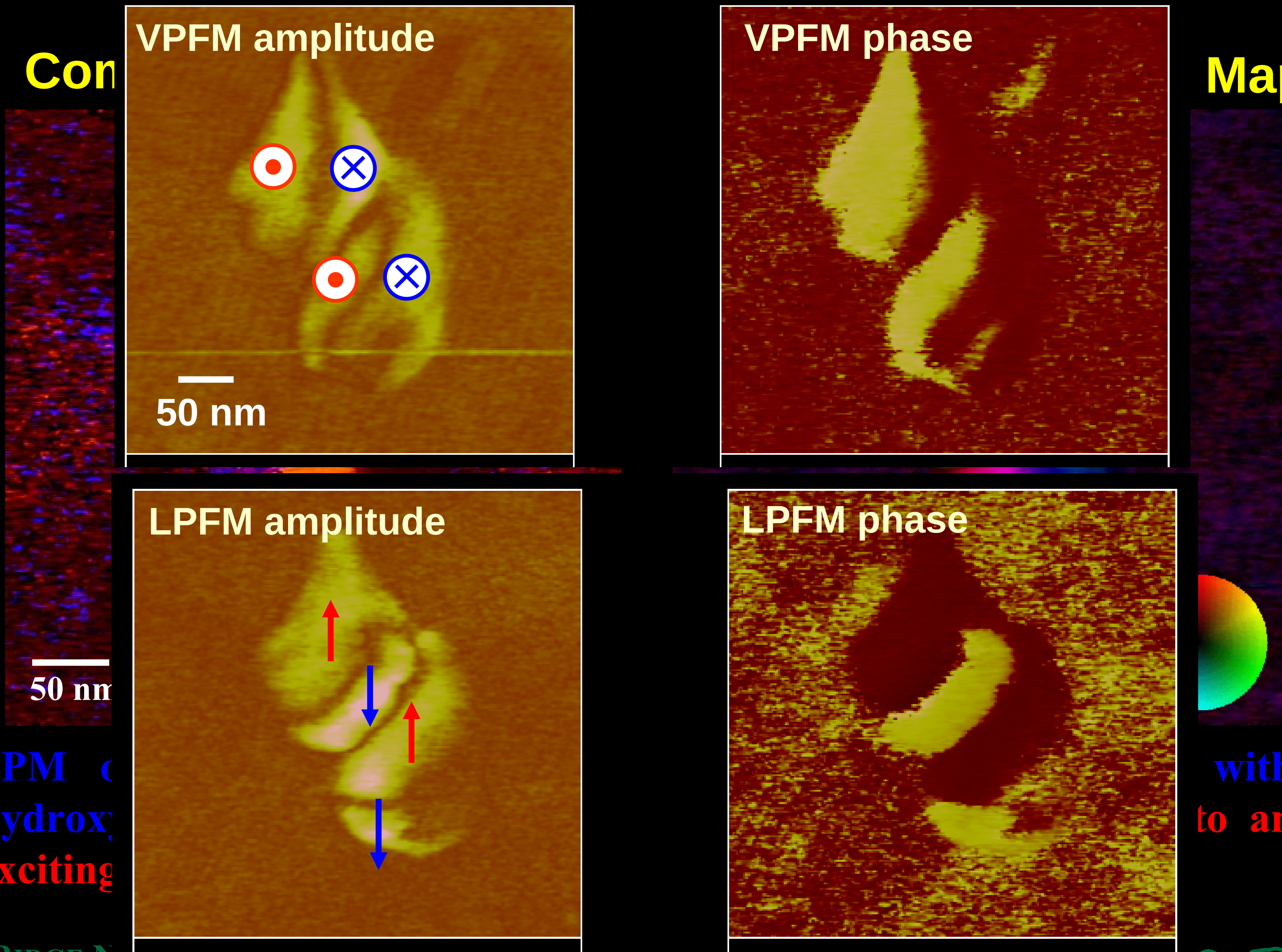

SPM c with
hydrox to an
exciting

Molecular Orientation from PFM Data

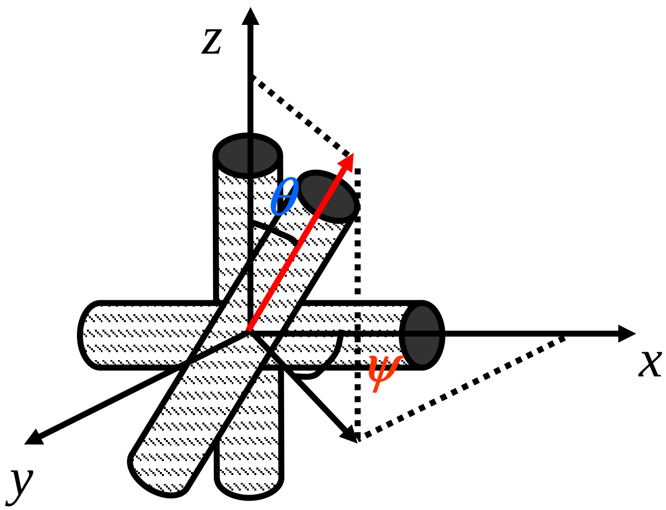

Semiquantitative Orientation Map for Collagen Fibril

Piezoresponse Surfaces for Collagen

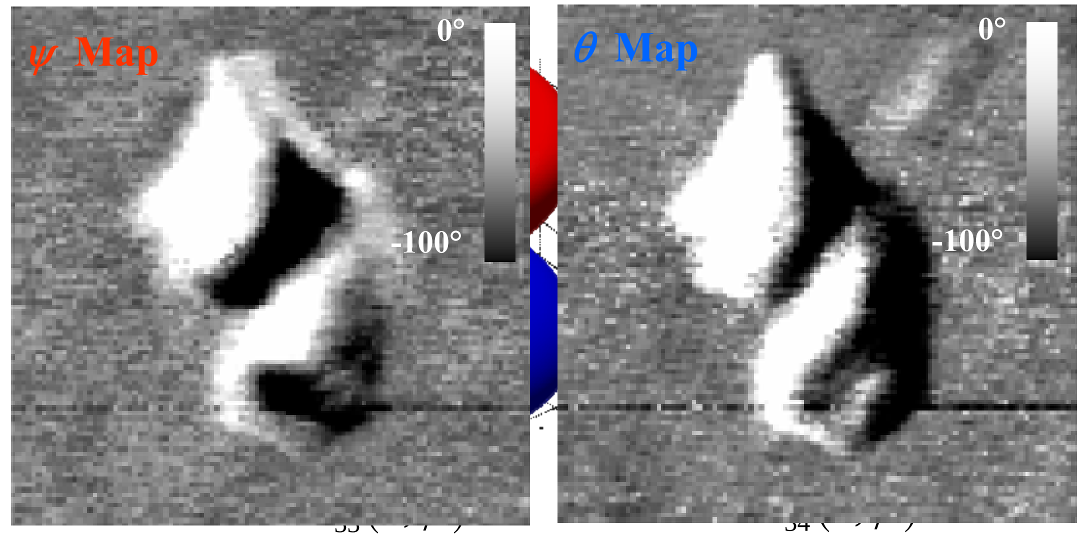

Tetragonal material (4mm):

$$\begin{pmatrix} 0 & 0 & 0 & 0 & d^0_{15} & d^0_{15} \\ d^0_{31} & d^0_{33} & d^0_{31} & d^0_{15} & 0 & 0 \\ d^0_{31} & d^0_{31} & d^0_{33} & d^0_{15} & 0 & 0 \end{pmatrix}$$

Vertical PFM

Lateral PFM (*x*)

Lateral PFM (y)

$$d_{ij} = A_{ik}(\phi,\theta,\psi)\; d^o_{kl}\; N_{lj}(\phi,\theta,\psi)$$

d_{ij} Piezotensor – lab coordinate system

d^o_{kl} Piezotensor – crystal coordinate system

$N_{ij}(\phi,\theta,\psi)$ $A_{ij}(\phi,\theta,\psi)$ Rotation matrices

Can we do it any other way?

Scalar

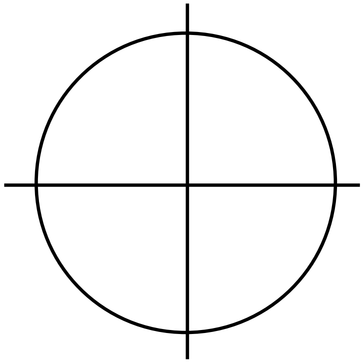

Temperature, Potential, etc.

2nd order tensor

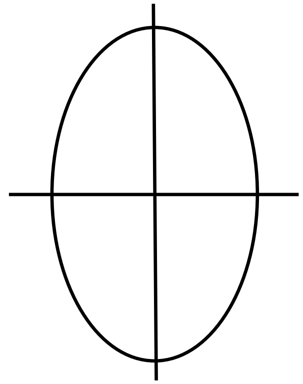

Dielectric constant Thermal conductivity

4th order tensor

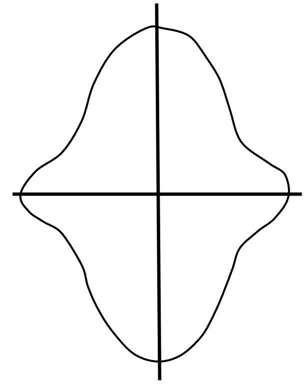

Elasticity, Kerr effect Electrostriction

Vector

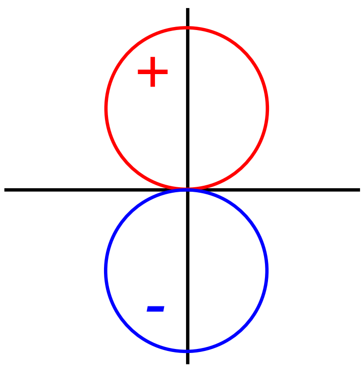

Polarization Magnetization Pyroelectricity

3d order tensor

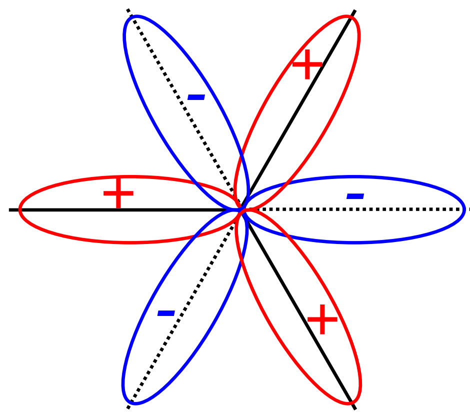

Piezoelectricity
Electrooptics, SHG

Orientation Imaging requires:

1. Rank 3 tensor property
2. High spatial resolution
3. Insensitivity to tip geometry or easy calibration

Piezoresponse Force Microscopy is perfect!

Ideally, we want to probe electromechanical behavior with ~1 pm/V sensitivity at ~0.1- 1 V excitation biases on molecular (biosystems) and unit cell (ferroelectrics) level.

Resolution Theory in PFM

5.2.1. Linear imaging theory
5.2.2. Transfer function, resolution and information limit
5.2.3. Phenomenological resolution theory in PFM
- lock-in effect
- resolution function
- image reconstruction

5.2.4. Analytical resolution theory in PFM
- Imaging domain walls and stripe domains
- Imaging cylindrical domains
- Effect of materials properties on resolution
- tip calibration

5.2.5. Implications for PFM data analysis
- statistical physics of domains
- domain wall width
- Writable domains
- Invisible domains

What is Resolution?

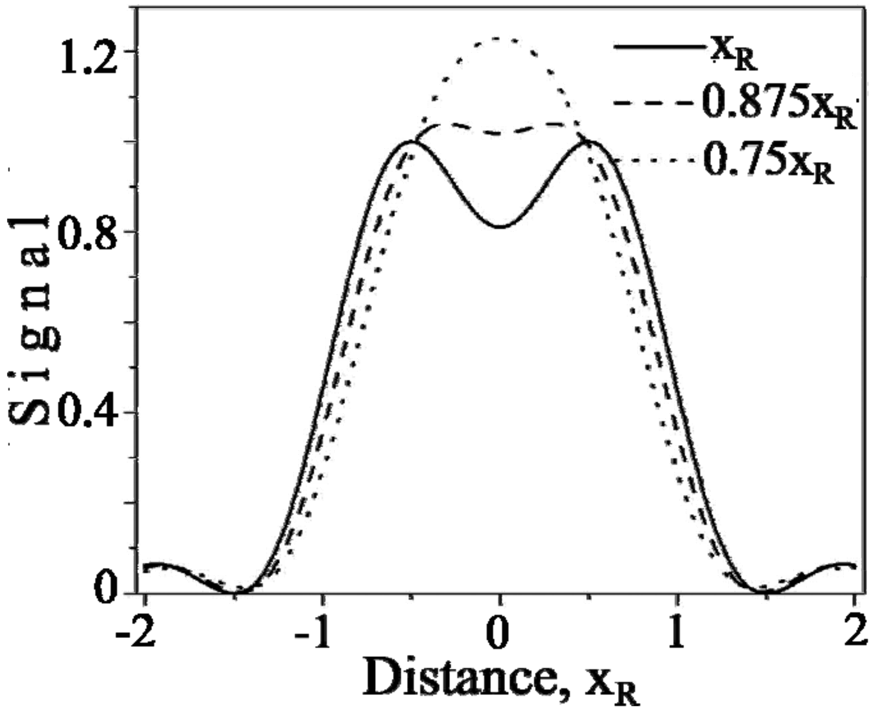

Optics: Rayleigh criterion

Transfer Function Theory

Real image always has contributions from probe and material

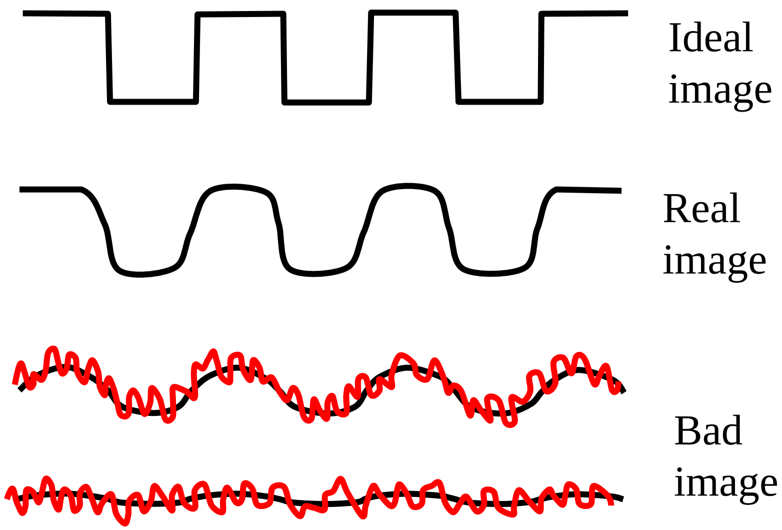

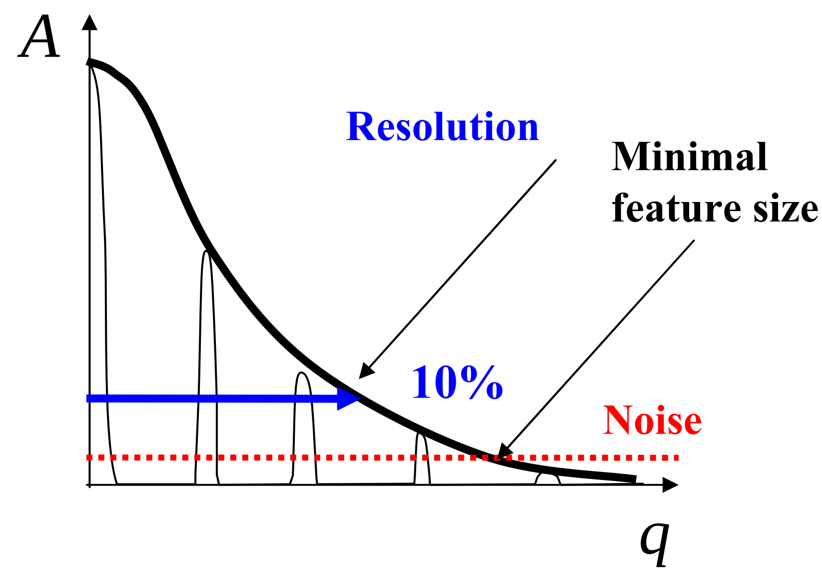

Linear Imaging Theory

Linear Imaging: $I(x) = \int I_0(x-y)F(y)dy + N(x)$

Ideal Image: $I_0(x-y)$

Real Image: $I(x)$

Transfer function: $F(y)$

Noise: $N(x)$

Fourier Transform: $I(q) = I_0(q)F(q) + N(q)$

Image Reconstruction: $I_0(q) = I(q)/F(q)$

- Ideal image has all Fourier components
- Transfer function decays for high k

We can define lateral resolution as:

- q for which TF = 0.1 TF (q=0)
- smallest feature we can detect:

$$I_0(q)F(q) = N(q)$$

Transfer Function Theory

$$\begin{tikzcd}[column sep=huge, row sep=huge]
\textbf{Ideal Image, } I_0(\mathbf{x}-\mathbf{y}) \arrow[r, "\text{Convolution with resolution function}", "\int I_0(\mathbf{x}-\mathbf{y})F(\mathbf{y})d\mathbf{y}"'] \arrow[d, "\text{Fourier Transform}"', "\int e^{i\mathbf{qx}}"] & \textbf{Experimental Image, } I(\mathbf{x}) \\
\textbf{Ideal Image, } I_0(\mathbf{q}) \arrow[r, "F(\mathbf{q})", "\text{Multiplication by object transfer function}"'] & \textbf{Experimental Image, } I(\mathbf{q}) \arrow[u, "\text{Fourier Transform}", "\int e^{-i\mathbf{qx}}"']
\end{tikzcd}$$

•Establish the resolution and information limits in PFM and its dependence on tip geometry and materials properties
• Develop the pathways for calibration of tip geometry
• Interpret the imaging and spectroscopy data in terms of intrinsic parameters
• Reconstruct the ideal image from experimental data,

Resolution in Transfer Function Theory

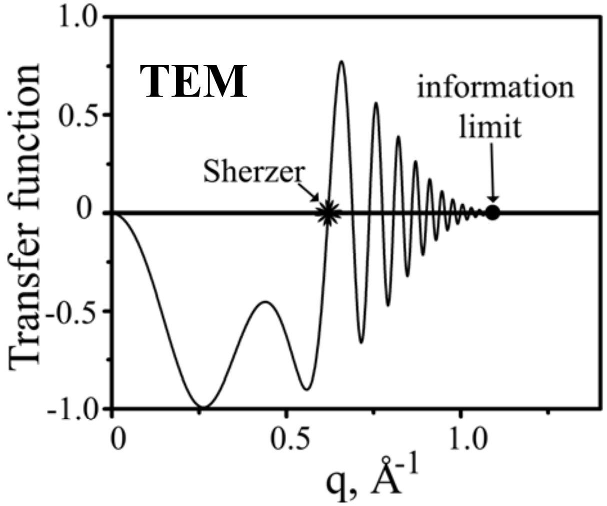

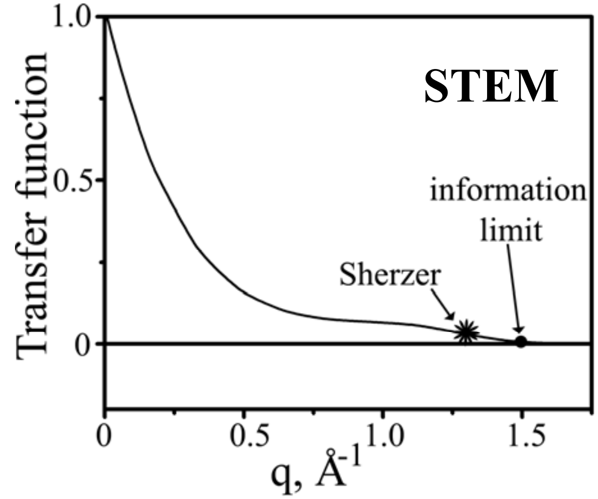

In electron microscopy, zeroes in transfer function define Sherzer resolution

Information limit corresponds to frequencies above which there is no information transfer

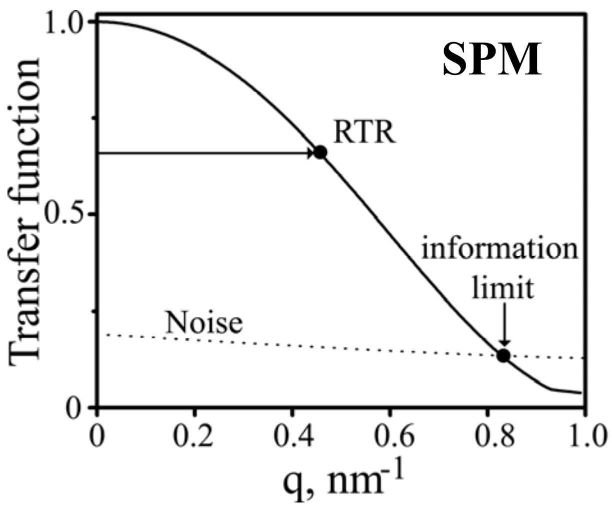

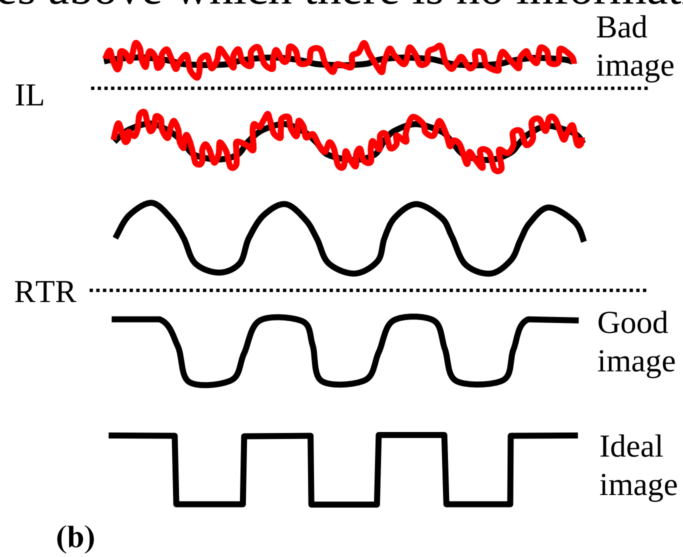

In SPM, there are usually no zeroes!

Resolution in PFM

In decoupled approximation, PFM image formation mechanism is linear if material is uniform in z-direction, $d_{mnk}(y-\mathbf{x}'', z) = d_{mnk}(y-\mathbf{x}'')$

PFM Image: $$u_3(\mathbf{0},\mathbf{y}) = \int_{-\infty}^{\infty} d_{mnk}(\mathbf{y}-\boldsymbol{\xi})F(\xi_1,\xi_2)d\xi_1 d\xi_2$$

Transfer function: $$F(\xi_1,\xi_2) = \int_{z=0}^{\infty} c_{jlmn}E_k(-\xi_1,-\xi_2,z)\frac{\partial}{\partial \xi_l}G_{3j}(\xi_1,\xi_2,z)dz$$

We calculate the resolution function in analytical form:

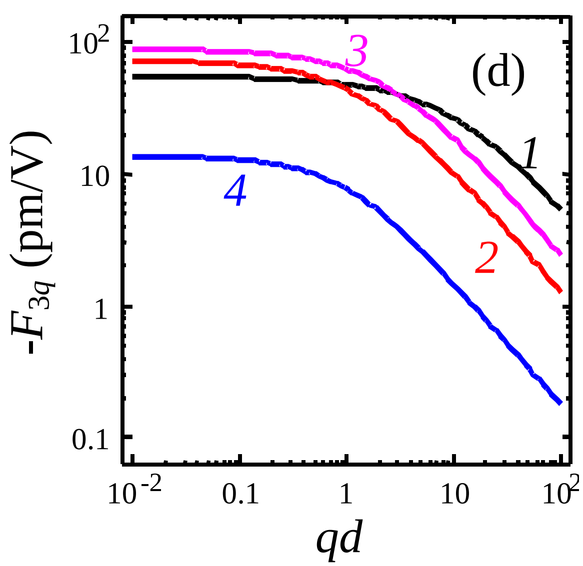

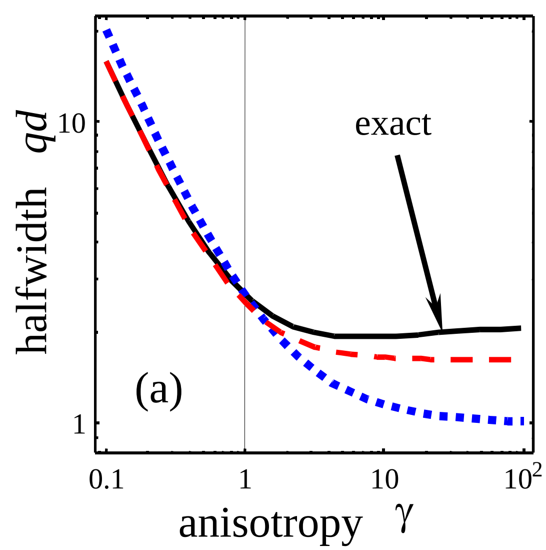

Point charge model

$$r_{\min} \cong \frac{\gamma\,\varepsilon_e R_0}{2\kappa}\frac{1+2\gamma}{(1+\gamma)^2}$$

Sphere-plane model

$$r_{\min} \cong \frac{\gamma\,\varepsilon_e R_0}{\varepsilon_e+\kappa}\frac{1+2\gamma}{(1+\gamma)^2}$$

Domain wall profile

Domain wall profile is a natural observable in PFM

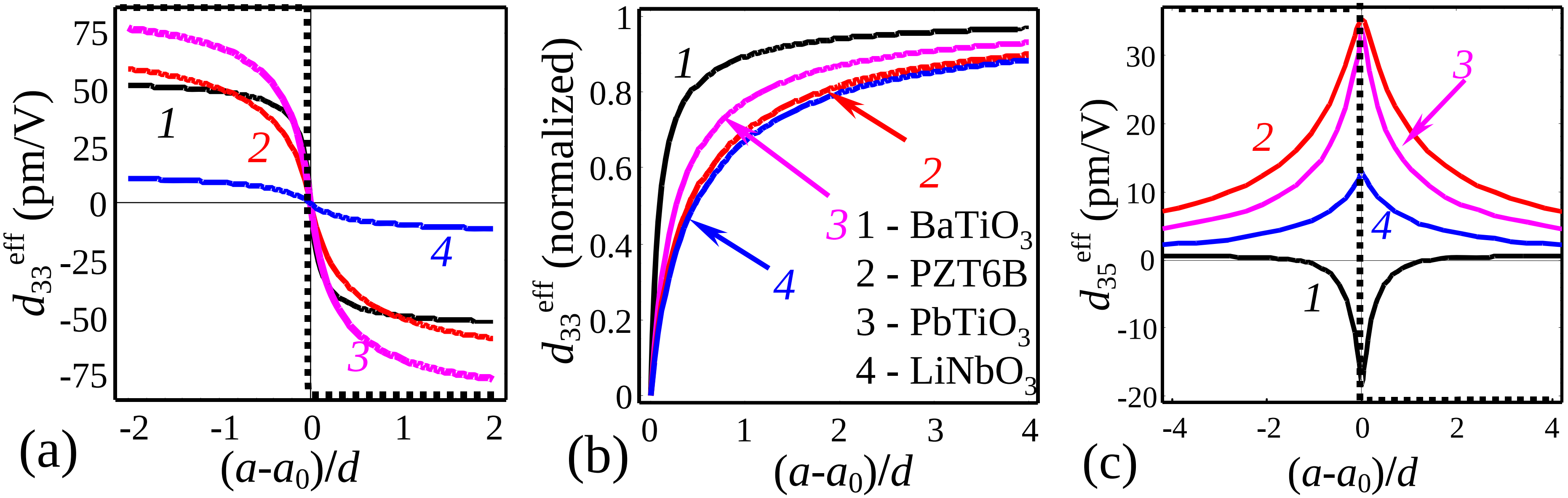

Vertical PFM

$$d_{33}^{eff} \approx d_{03} + \left[\frac{3}{4}\left(d_{33} + \left(\frac{1}{3} + \frac{4}{3}\nu \right) d_{31} \right) \frac{s}{|s| + 1/4} + \frac{1}{4} d_{15} \frac{s}{|s| + 3/4} \right]$$

Lateral PFM

$$d_{35}^{eff} \approx d_{01} + d_{33} \frac{3/8}{1 + 3|s|} + d_{31} \left(-\frac{3/8}{1 + 3|s|} + \frac{1 + \nu}{1 + 4|s|} \right) + d_{15} \frac{2/\pi - 3/8}{1 + (8/\pi - 3/2)|s|}$$

We can use domain wall profile to calibrate the tip!

Tip Calibration in PFM

We can determine tip parameters by fitting domain wall profile using model of superposition of point charges

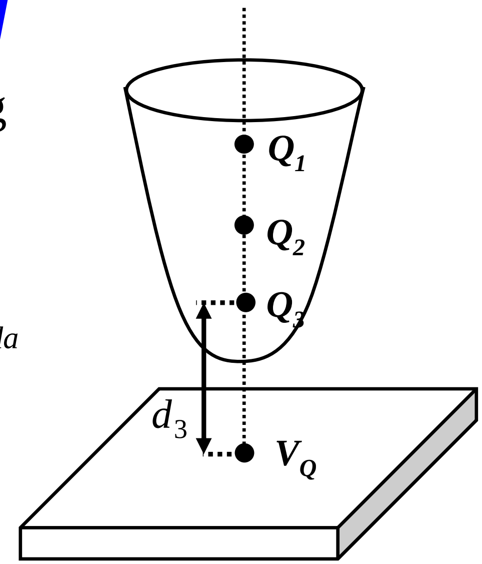

$$F[u_3]=\int\left(PR(a)-\frac{1}{2\pi\varepsilon_0(\varepsilon_e+\kappa)}\sum_{m=0}^{N}\frac{Q_m}{d_m}\left(g_{313}\left(\frac{a-a_0}{d_m},\gamma,\nu\right)d_{31}+g_{351}\left(\frac{a-a_0}{d_m},\gamma\right)d_{15}+g_{333}\left(\frac{a-a_0}{d_m},\gamma\right)d_{33}\right)\right)^2 da$$

Material	ε_e	Width, nm	Q	d , nm
$LiNbO_3$	1	96	1000	92
Epitaxial PZT	1	107	2550	125
PZT in air	1	58	723	86.5
PZT in liquid	80	6	104	11.8

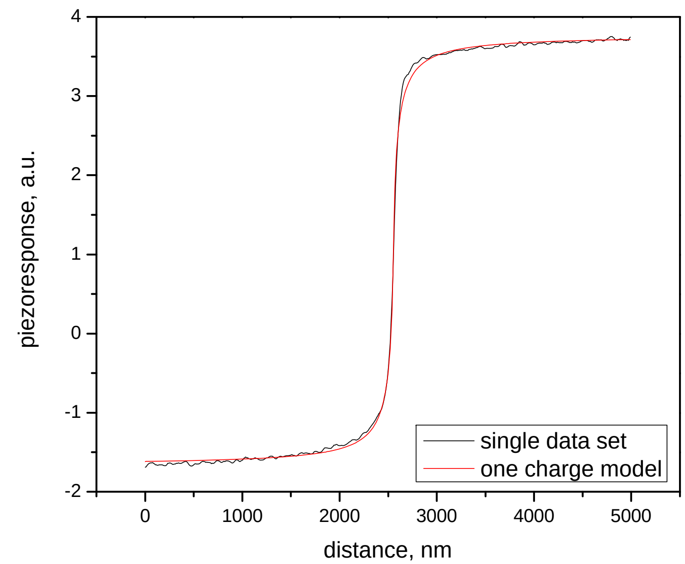

Surprisingly, single charge provides good description

Why is Tip so Large?

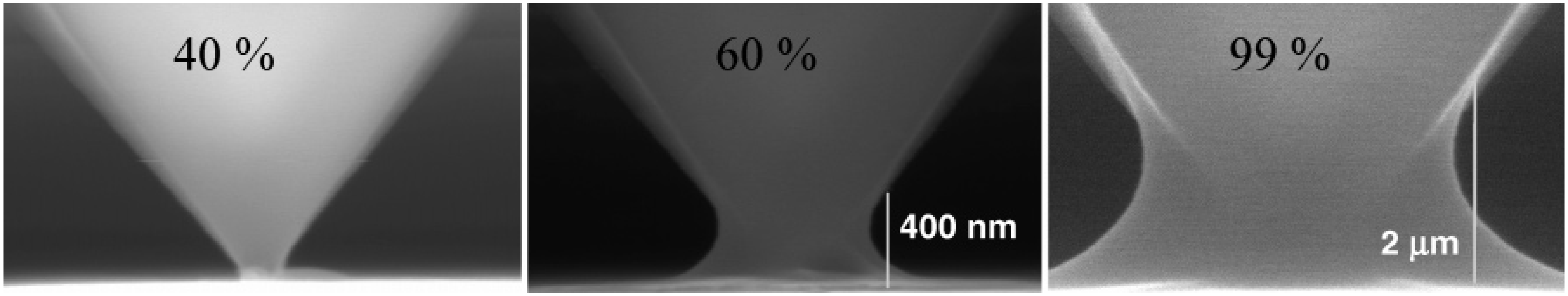

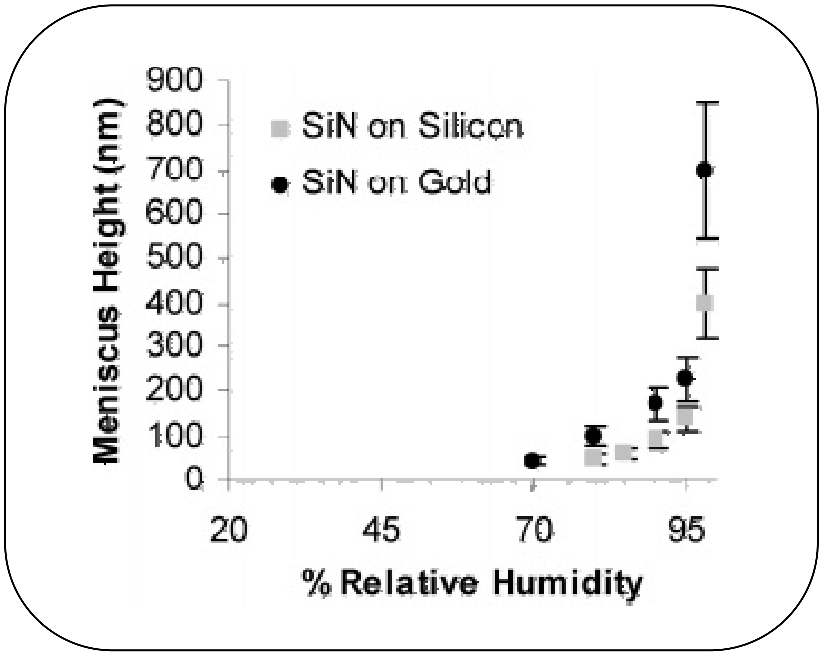

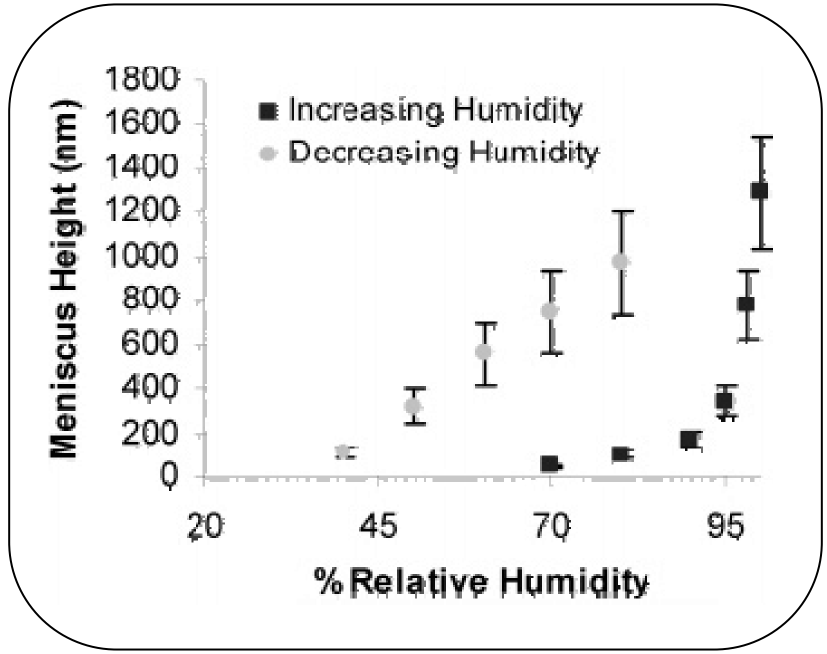

Langmuir **21**, 8096-8098 (2005)

Effect of finite resolution on imaging

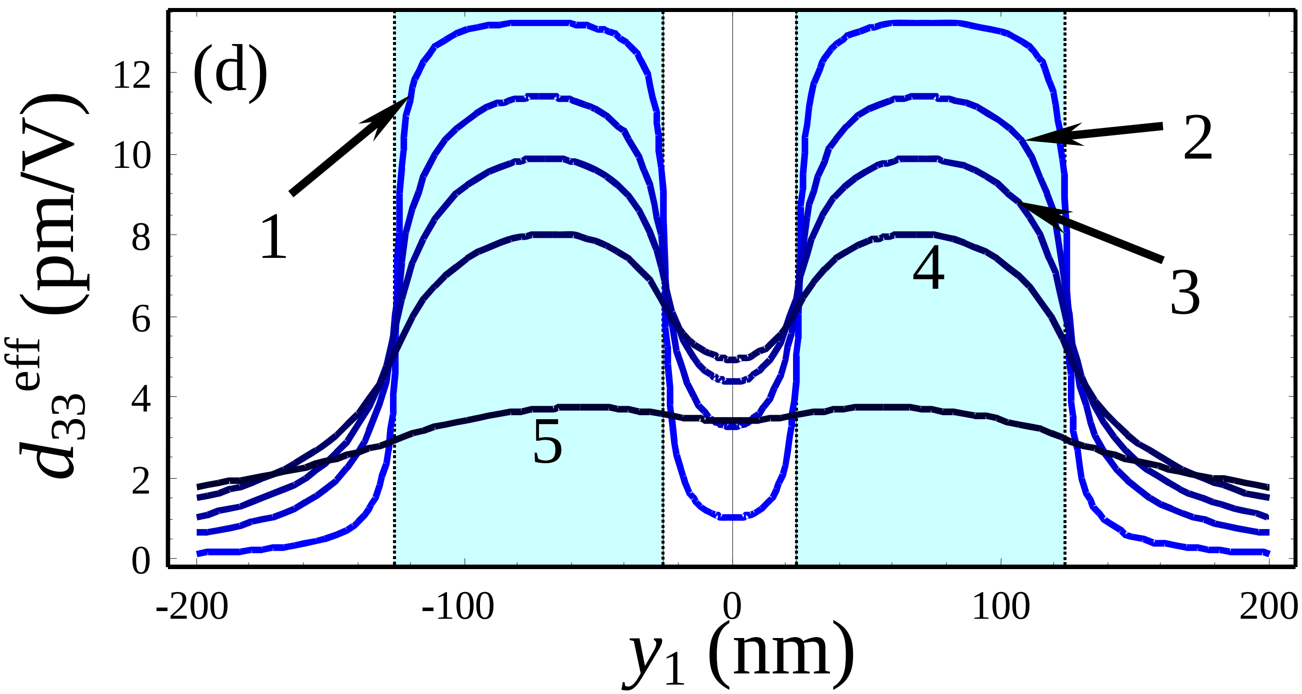

- For low resolutions, domains are difficult to distinguish
- Signal in the center of domain decreases
- However, the domains are always visible

Periodic Domain Structures

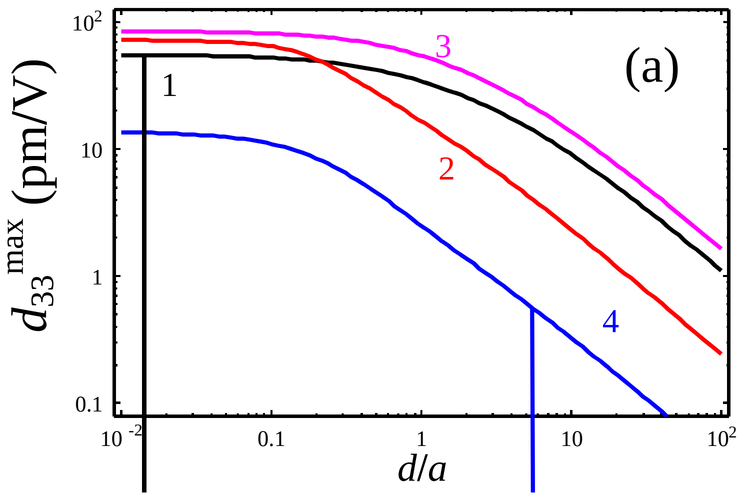

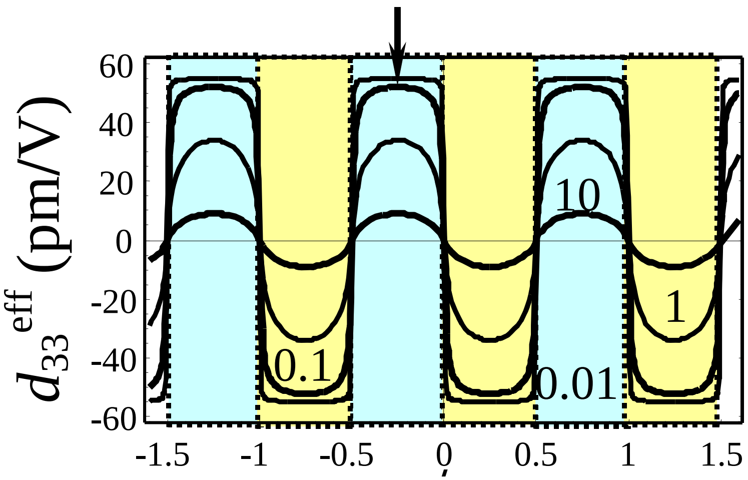

Ideal Image

$$d_{klj}(\mathbf{y}) = d_{klj} \sum_{n=0}^{\infty} \frac{4}{(2n+1)\pi} \sin\left(\frac{2\pi}{a}(2n+1)y_1\right)$$

Real Image

$$u_3(a, y_1) = \sum_{n=0}^{\infty} \frac{4}{(2n+1)\pi} \sin\left(\frac{2\pi}{a}(2n+1)y_1\right) F_q\left(\frac{2\pi}{a}(2n+1)\right)$$

For low resolution, only one component survives:

$$u_3(y) = \frac{4}{\pi} \sin\left(\frac{2\pi y_1}{a}\right) F_q\left(\frac{2\pi}{a}\right)$$

Information Limit

The smallest visible feature size is determined by the noise level of the system

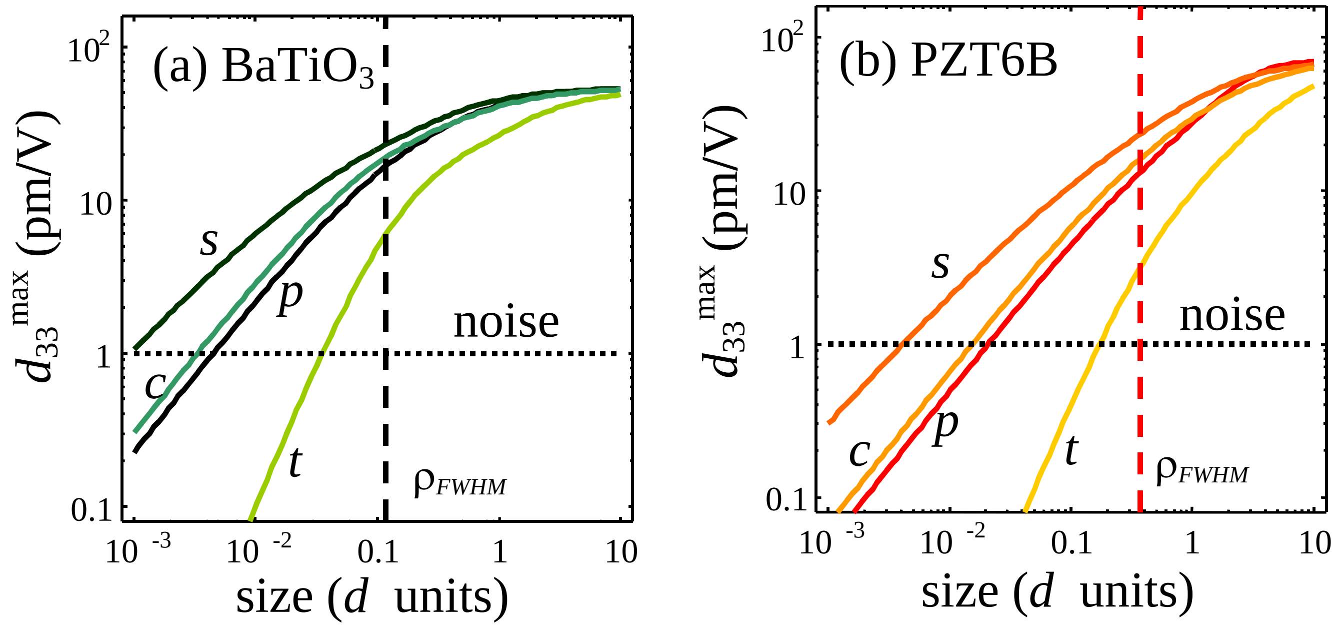

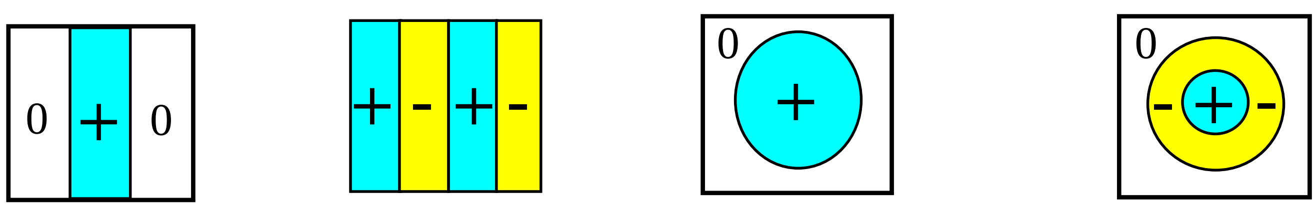

single stripe (s) size=a/d

periodic stripes (p) size=a/d

cylinder (c) size=r/d

nested cylinders (t) size=r_o/d

Information Limit

Raleigh resolution in phase image is equal to information limit in mixed signal image

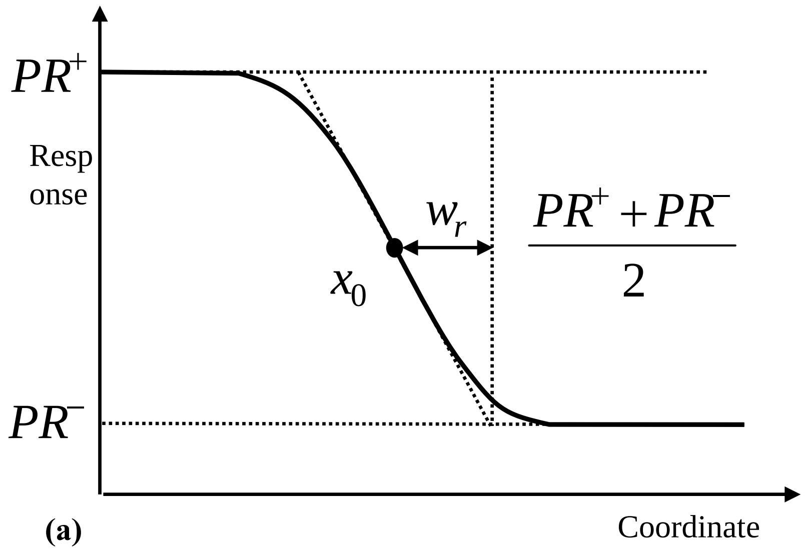

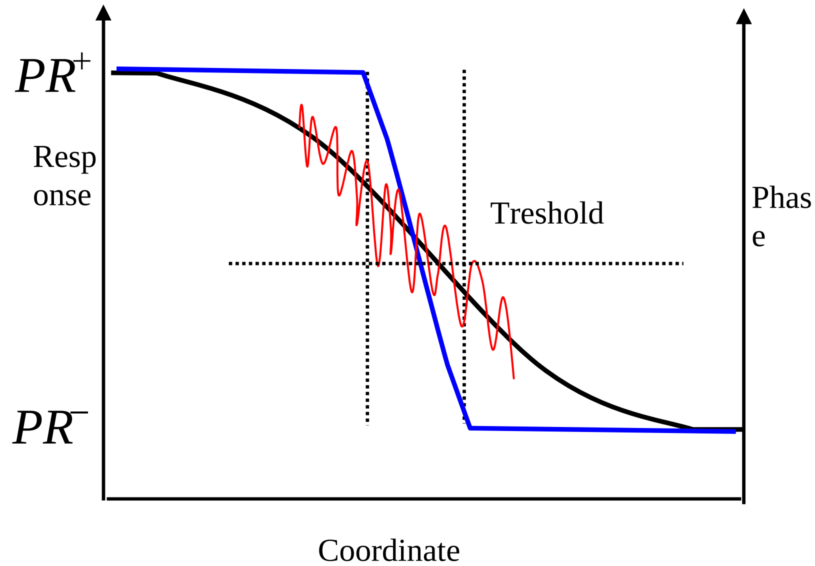

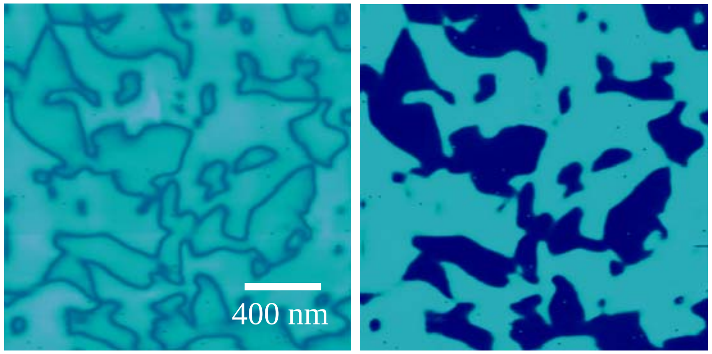

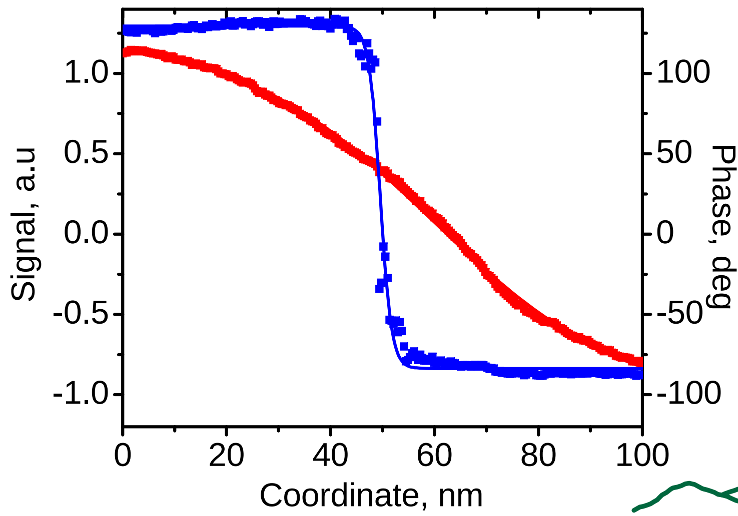

Lock-In Effect on Imaging

Time in each point ~ 4 ms

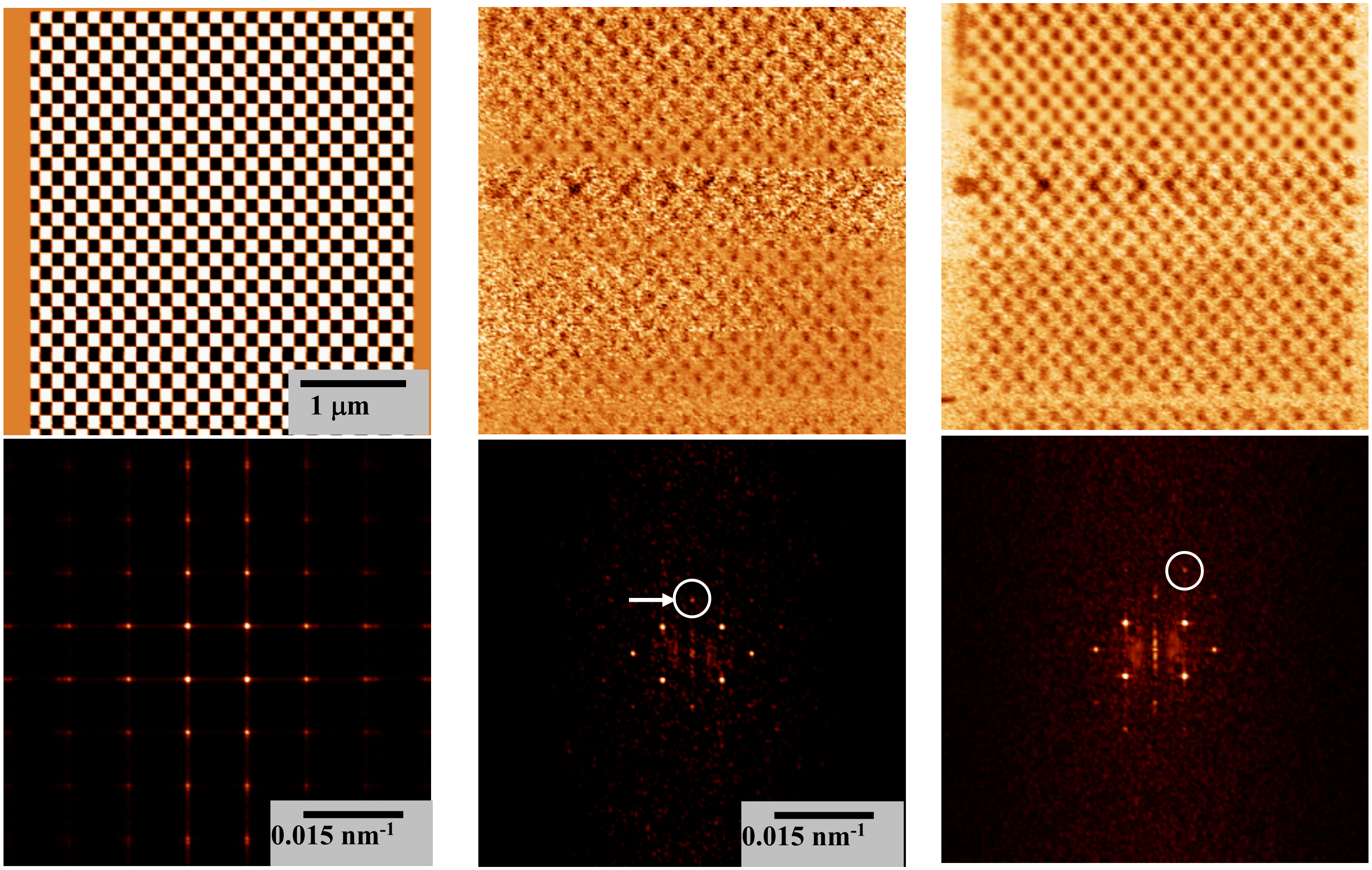

Ideal Image | 0.5 ms | 1 ms

Lock-In Effect on Imaging

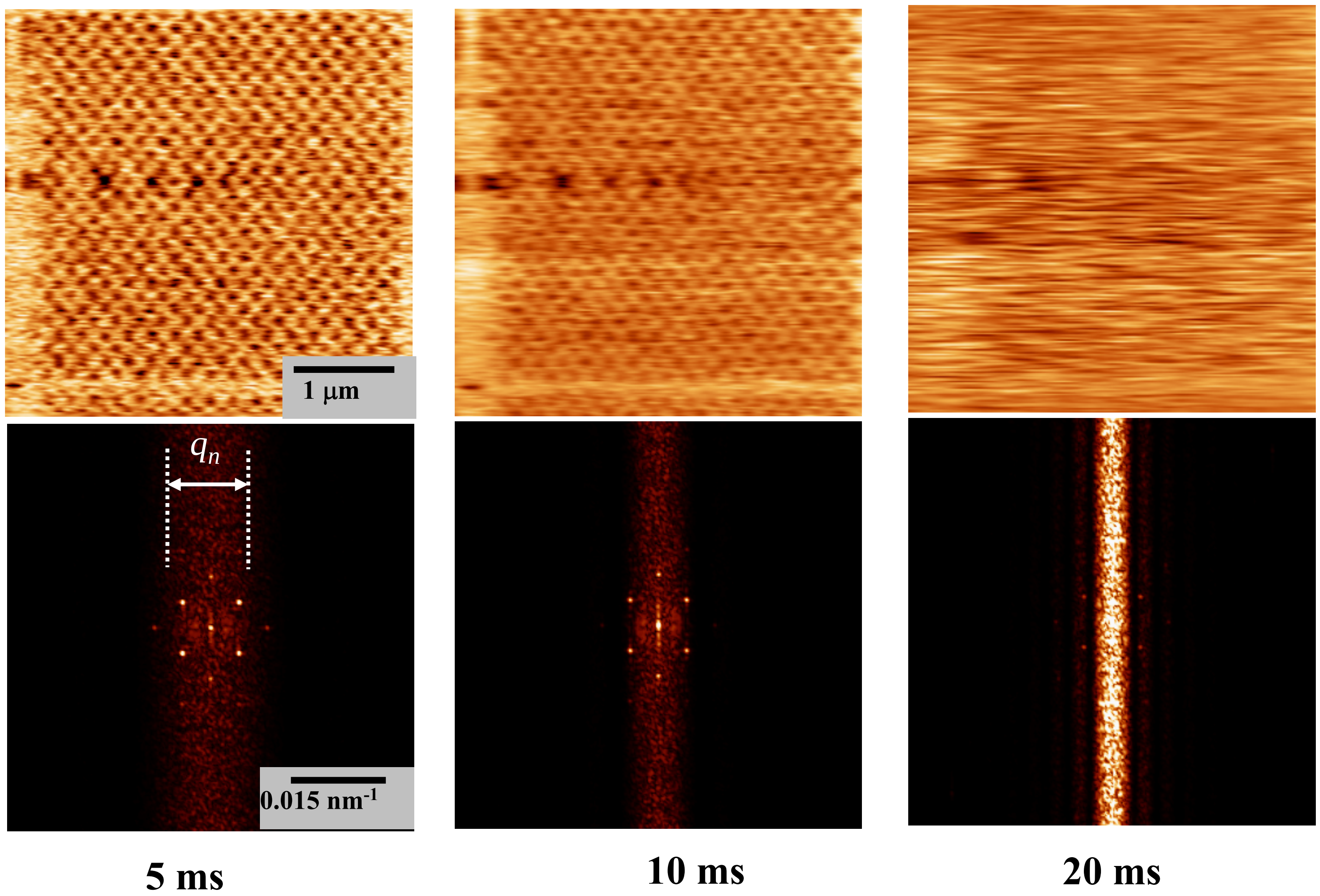

Lock-In Effect on Imaging

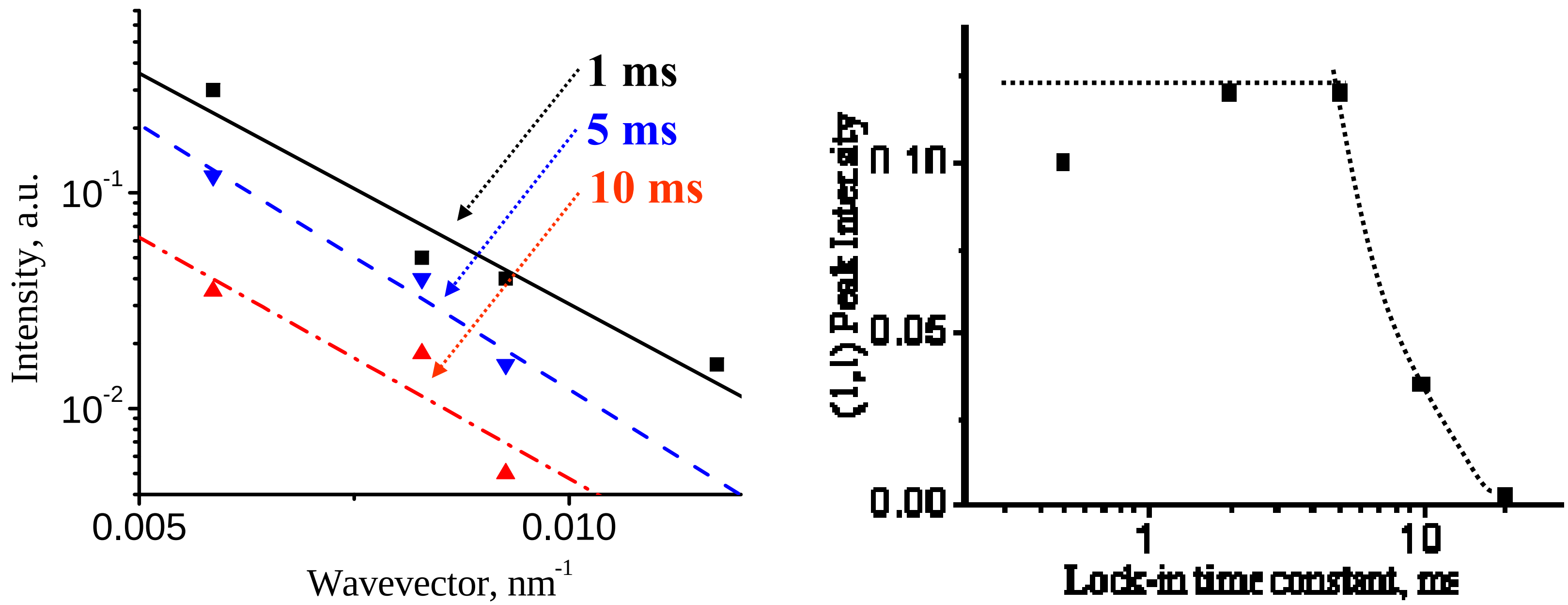

The wavevector dependence of peak intensity: $I(hk) = I_0 \exp(-q/G)$

Resolution function is a product of lock-in and tip parts: $F(\mathbf{q}) = F_{tip}(q)F_{la}(q_x)$

For small time constants $\tau << \tau_{pixel}$ we have $F_{la}(q_x) = 1$ but $N(q) \sim \sqrt{\tau_{pixel}/\tau}$

For large time constants noise is small, but image is streaky

Application of Linear Imaging Theory to PFM

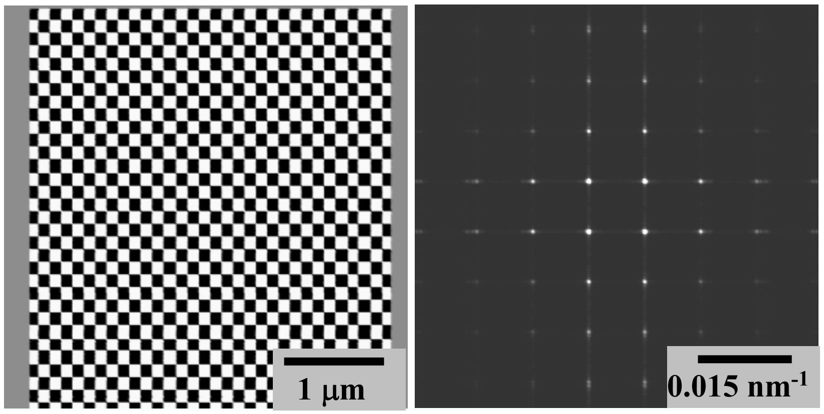

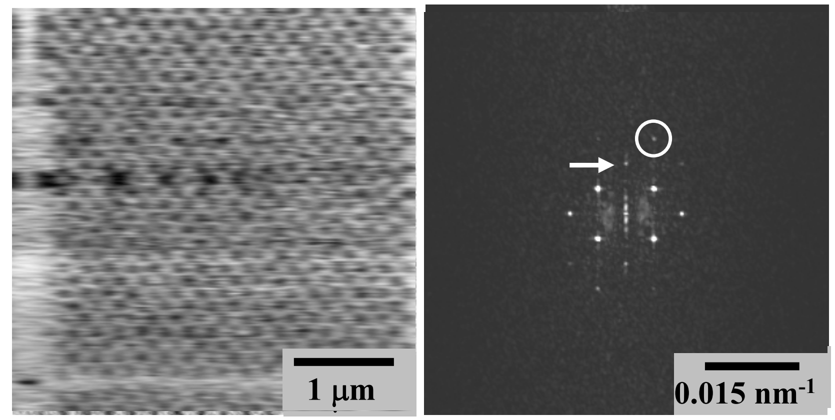

Checkerboard standard

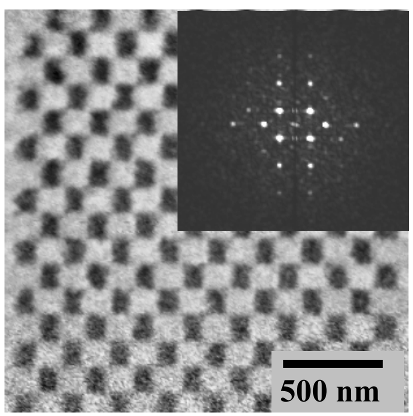

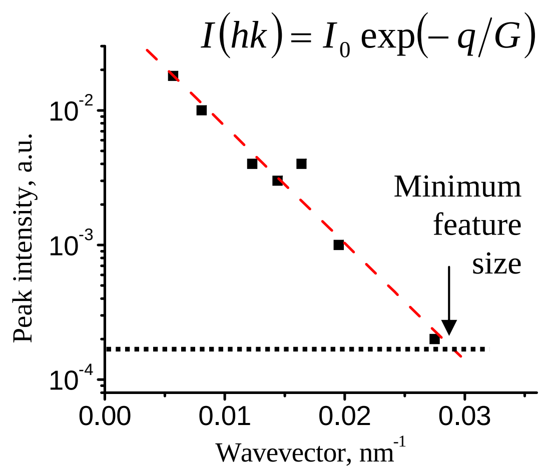

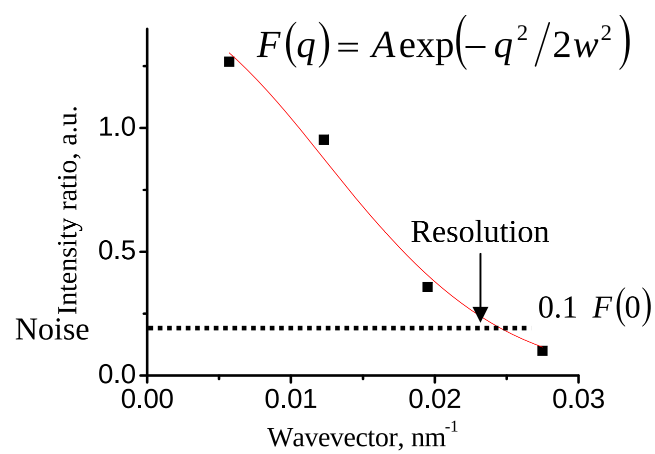

Transfer Function and Image Reconstruction

Variable mesh size standard

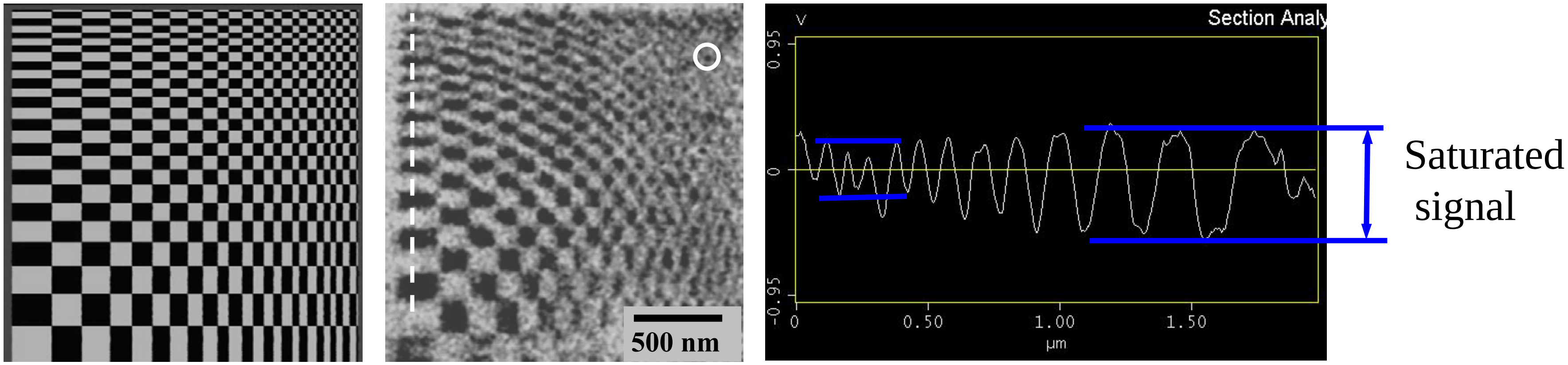

Image reconstruction using transfer function

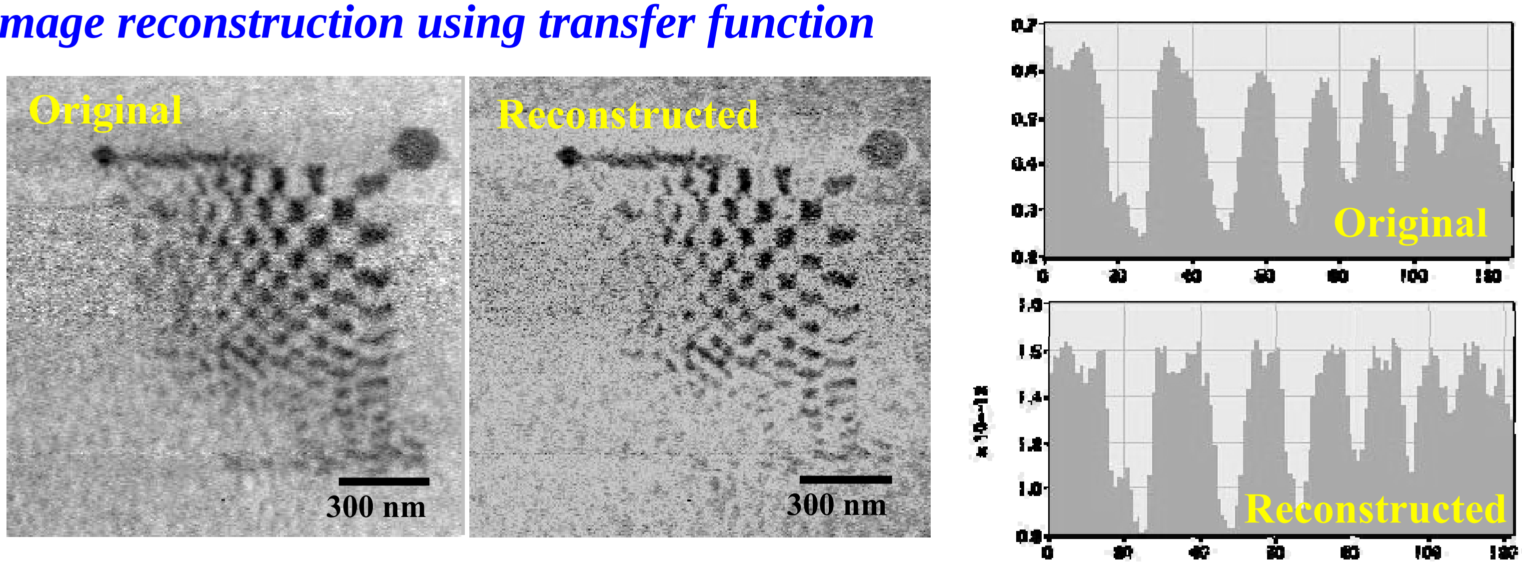

- Variable mesh size standard allow determination of minimal writable/detectable domain size
- Checkerboard standard allows resolution to be determined
- For epitaxial PZT film, minimum domain size is determined by resolution, rather then writing process
- Using known transfer function, PFM image can be reconstructed from experimental data.

Transfer Function and Image Reconstruction

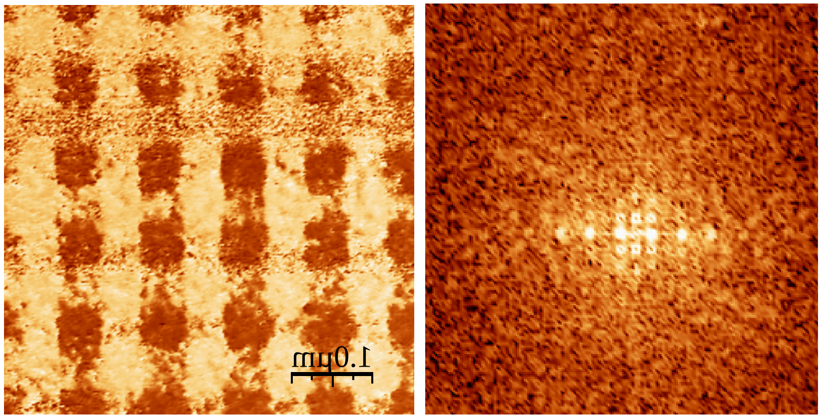

For sol-gel and inhomogeneous films, minimum domain size can be much larger then resolution as controlled by microstructure

Image reconstruction using transfer function

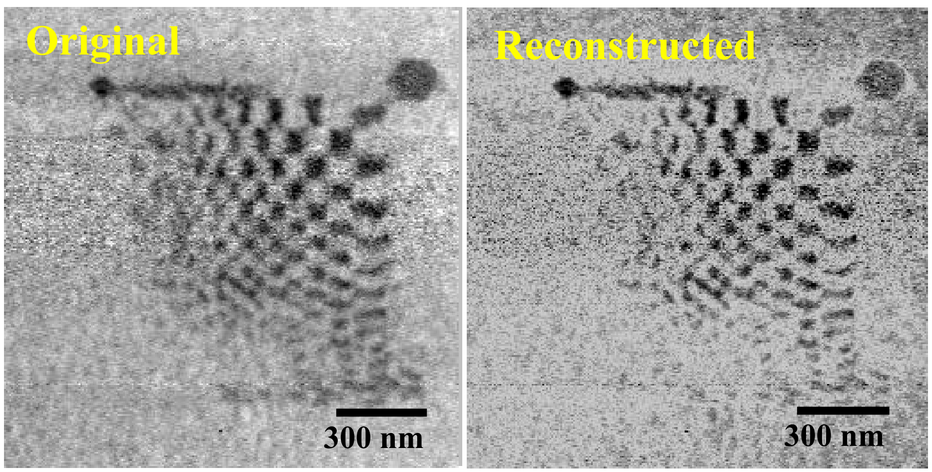

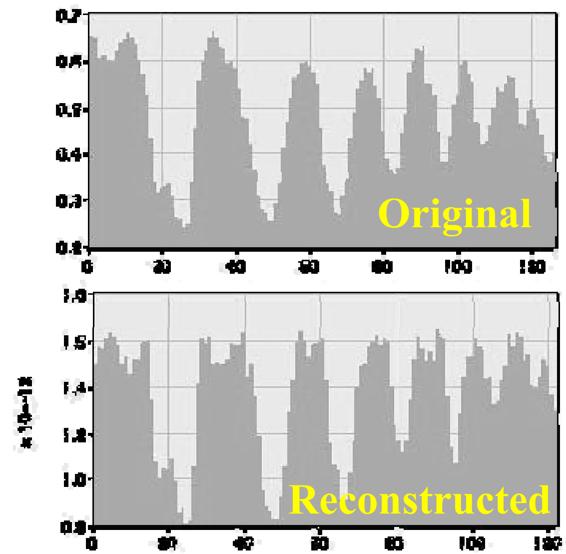

Using known transfer function, PFM image can be reconstructed from experimental data.